SIMULATION MODELING OF A VENTED DEFLAGRATION

BY

ARIEL LAZARO

A thesis submitted to the Faculty of Graduate Studies
in partial fulfillment of the requirements for the degree of

MASTER OF SCIENCE

Department of Mechanical and Manufacturing Engineering
University of Manitoba
Winnipeg, Manitoba

December 2007

THE UNIVERSITY OF MANITOBA

FACULTY OF GRADUATE STUDIES

*****

COPYRIGHT PERMISSION

SIMULATION MODELING OF A VENTED DEFLAGRATION

BY

ARIEL LAZARO

A Thesis/Practicum submitted to the Faculty of Graduate Studies of The University of Manitoba in partial fulfillment of the requirement of the degree

MASTER OF SCIENCE

Abstract

Intentional ignition is an effective technique for mitigation of hydrogen concentrations during a loss of coolant accident (LOCA). This reduces the possibility of detonation reaction by maintaining combustion to the subsonic deflagration regime. Without sufficient venting, deflagration pressures can reach hazardous levels. The focus of this research was the development of a code being capable of visualizing flame movement of vented deflagrations while predicting pressures produced. The simulation was constructed using a flame tracking concept based on laminar burning, thermal expansion and vent induced turbulence. Results are compared to experiments conducted at the AECL (Atomic Energy of Canada Limited) Large Scale Vented Combustion Facility, as well as simulated results by existing code. The predicted peak pressures were generally lower than the comparison data. Burn times were also much slower, suggesting insufficient simulation of vent effects. Vent size correlation demonstrated a decrease in pressure as vent size increased. Further examination considered the effects of ignition location on peak pressure, with central ignition providing the highest pressure values. The simulation is concluded to create an effective foundation for combining the governing concepts of vented deflagration with suggested areas of improvement.

Acknowledgements

Thanks must be given to Dr. Chan and the members of the hydrogen group at AECL-Pinawa, for providing an opportunity to conduct research at their sides. They are to be commended for dedication in the face of uncertainty. The guidance of Dr. Chan provided the foundation for all combustion based research.

Doyle Buhler and Kurt Buhler, along with Jim Pendergrass must be thanked for the opportunity and support while conducting research for the Venture 2 Initiative. Their inventiveness and drive for innovation helped to create an enjoyable, eye-opening experience.

I extend my gratitude to AECL, Imbibo and NRC-IRAP for providing financial support during the course of their respective projects. Their commitment was invaluable in building my own confidence by emphasizing the significance of the work.

Most importantly, I must thank Dr. Peng. His patience is endless in his willingness to continue to guide me.

Table of Contents

Nomenclature

m_b	Mass of burnt gas
m_u	Mass of unburnt gas
m_τ	Mass of total gas
m_v	Mass of venting gas
m_{uv}	Mass of unburnt venting gas
m_{bv}	Mass of burnt venting gas
ρ_b	Density of burnt gas
ρ_u	Density of unburnt gas
ρ_{bv}	Density of venting burnt gas
ρ_{uv}	Density of venting unburnt gas
S	Burning velocity
S_t	Laminar burning velocity
S_v	Burning velocity cause by vent effect
P_a	Atmospheric pressure
P	Pressure
V_b	Volume of burnt gas
V_u	Volume of unburnt gas
V_o	Initial gas volume
A	Flame surface area
γ_b	specific heat ratio of burnt gas
γ_u	specific heat ratio of unburnt gas
γ	specific heat ratio of gas
C_d	Venting Co-efficient
A_v	Vent Area
W	Thermal expansion ratio
t	Time
R	radius of flame sphere
$\vec{R}$	flame tracking vector
$\vec{V}$	exit velocity at vent

List of Figures

Chapter 1:
Introduction

Vented deflagration is a form of combustion that remains in the subsonic regime. In energy producing facilities, such as nuclear power plants and oil drilling stations, a subsonic burn creates a lower risk than a supersonic burn, otherwise known as a detonation. The main risk is the tremendous increase in pressure that a detonation produces when compared to a deflagration. That is not to say that a deflagration is not a threat. Depending on how the burn progresses, the pressure produced can still reach critical levels.

The focus of this research is the development of a combustion simulation to replicate vented deflagration in large volumes. The simulation is meant to estimate pressure development and create visualization of the flame growth during a deflagration.

Sophisticated software is available for fluid and combustion analysis. The purpose of this research is not to compete with fully developed software. It is hoped that the simulation first and foremost be a learning aid, providing an understanding for the general behavior of vented deflagrations. Visualization software will be used to create a graphical representations of the data produced.

1.1. Background

LOCA and Mitigation

A LOCA, or a loss of coolant accident, poses serious threat to the overall integrity of the CANDU (Canadian Deuterium Uranium) nuclear facility. A particular concern is the sudden release of a high temperature gas mixture containing hydrogen, into the interior of the facility. During a LOCA, hot water vapors can react with fuel cladding zirconium

alloy to produce hydrogen gases [1, 2]. A volatile gas mixture is generated as the hydrogen combines with the available air.

As the hydrogen levels increase, the risk to the integrity of the containment structure increases. To prevent the collection of this mixture into hazardous concentrations a number of mitigation techniques are used [3]. Available methods for reducing risk include the release of inert gases or excessive steam levels to reduce the volatility of the hydrogen-air mixture. Recombiners are also employed to integrate the hydrogen and oxygen into water. An effective mitigation method for large volumes filled with volatile gases, is the intentional ignition and venting of the gas mixture, before it can reach dangerous levels. This intentional burn is meant to keep combustion controllable with acceptable pressure levels [4]. Intentional burning and venting are effective methods for mitigation. Still, careful use of the technique must be practiced to avoid other potentially hazardous situations.

DDT

A deflagration is a subsonic burn, a detonation is a supersonic burn that carries immensely high pressures. Igniters are used for mitigation with the intention of inducing deflagration combustion. Turbulent effects caused by the vent and internal obstacles can cause the deflagration flame to accelerate into the supersonic regime triggering a detonation [4]. This combustion phenomenon is otherwise known as a DDT, or a deflagration to detonation transition. In some cases the overall pressure of a DDT can be greater than that of a direct detonation [5].

For a DDT to occur, hydrogen, steam and air mixture must be provided with sufficient acceleration properties and burning distance for a detonation to occur. Generally, the higher the concentration of hydrogen, the shorter the distance required. This of course provided that there is enough oxygen available to sustain burning.

GOTHIC (Generation Of Thermal-Hydraulic Information for Containments) is a thermo hydraulic code used at AECL (Atomic Energy of Canada Limited) to simulate the

hydrogen collection patterns within the containment of a CANDU facility [6]. DDTINDEX developed at AECL, uses data from these simulations estimating hydrogen, air and steam concentrations throughout the test volumes. Comparing data collected from experiments and existing models, DDTINDEX analyzes the gas mixture to predict the possibility of a DDT based on the flame acceleration properties of the gas and the distances required to produce a DDT. Appendix A provides information relating to the graphical development of the DDTINDEX data.

Vented Deflagration

A deflagration produces far lower over pressures than a detonation. That is not to say that deflagration pressures cannot be dangerous. Deflagration pressure still present potential risks to equipment and containment. Venting practices are used to relieve both pressure effects from deflagration as well as allowing volatile gas mixtures to escape. Adequate relief is only offered when sufficient venting is used. Experiments and models have been developed to both test for the effects of vented deflagration and predict safe venting practices.

1.2 Literature Review

Testing and Experiments

The hydrogen research group at AECL established experiments examining the behavior of hydrogen [7]. All experiments were geared to help developing procedures for safe mitigation practices during CANDU accident scenarios [8].

The collection of experiments tested various aspects of hydrogen behavior. Gas concentrations, distributions, and other physical properties prior to ignition were examined to understand the conditions necessary to create and sustain combustion. Other experiments considered properties during combustion, including the mechanisms that accelerated flame speeds and the properties required for a DDT.

One facility housed a 2.3 m diameter sphere for use in various combustion experiments. Kumar et al [9] would use the arrangement to carry out vented combustion experiments. Their work would explore the effect of varying vent sizes and ignition location on overall combustion behavior, specifically in terms of pressure development and burn times. Their results were compared to models which had previously been developed [10].

Another component of the vented deflagration research conducted at AECL was the Large Scale Vented Combustion Test Facility, or the LSVCTF [11]. The LSVCTF was designed to generate combustion data in volumes resembling actual rooms, both in scale and shape. The LSVCTF provides a large rectangular test volume measuring $120m^3$, which is configurable to create varying confinement parameters. It was built as a multipurpose facility for testing numerous properties critical to containment safety.

Outside of AECL, Sato et al [12] have conducted hydrogen deflagration experiments using combustion vessels of varying scale and geometry. Rectangular, spherical and cylindrical arrangements have been used to test the effects of varying hydrogen concentrations, the effect of scale and the effect of obstacles on flame velocity and pressure generation.

Molkov et al [13] compiled their own previous research in deflagration behavior along with research by other groups, including that of the AECL group. Their comparisons examined the similarities in the handling of either hydrogen or hydrocarbons in vented deflagration. Other researcher conducted by Molkov includes both combustion experimentation, simulation as well development of venting apparatuses. One set of experiments examined the correlation between combustion behavior and vent size [14].

Models

Motivated by a need to provide safe venting areas, Bradley et al [15] hypothesized a method using idealized situations. A key component of their work was to consider a spherical combustion chamber. This combined with a perfectly centered ignition would create optimal conditions for worst case analysis.

As a deflagration flame grows, pressure is generated at the flame front. This effect is quenched when a flame front is extinguished by a volume wall or obstacle. Under their assumed conditions a deflagration flame will grow outwards and equally in all directions, thus creating a sphere. The experimental setup would allow the flame to grow unobstructed to the maximum size of the spherical vessel, with all flame fronts actively propagating until all are quenched simultaneously. While, completely unrealistic, this arrangement ensures a maximum pressure effect for the volume.

The volume begins as an unvented structure. A vent of a specified size is opened when it is forced open by the pressure generated by the combustion. The vent opens at a specified level of force. An established venting theory would be used to develop the relationships necessary for the determination of the maximum pressure produced under the various possible conditions.

Bradley et al [15] introduced a value that would compare the geometric properties of the vessel and vent along with burning velocities of the gas. These solutions would then be used to verify whether vent sizes were sufficient and estimate vent size requirements. Their work would go further with the development of a code based on the assumptions of the aforementioned research [16].

Building up on the idea of a spherical flame growth was the work of Mulpuru and Wilkin [10]. Where Bradley assumed a spherical flame in a spherical vessel, Mulpuru took the flame assumption into different geometries. This would include a sphere with different ignition points, and a cylinder with varying ignition points.

Their approach is similar to Bradley et al [16], using the same established vented combustion theories. The difference was that because of the geometric conditions chosen, the flame front would not quench simultaneously. Rather portions of the assumed spherical flame wall would be intersected by the volume geometry.

Indicating that pressure is only created at the flame wall, the critical portion of their work was the calculation of the active flame wall. Their results agreed with existing test results in a more qualitative manner. As specified conditions were varied, the expected change in reaction and overall pressure rise would follow in the appropriate manner. The culmination of their work was the computer code VENT.

Swift [17] considered a similar geometric model. In closed volume circumstances the spherical assumption would hold. Swift suggests that in vented situations, an elliptical shape should be adopted to account for the accelerated flame growth toward the vent. Swift [18] continued by examining the role of the geometric deflagration models in the practical application of combustion venting.

Fairweather et al [19] maintained developments in the geometric modeling of deflagration. Their model would present a flame geometry that would begin as a sphere in a rectangular vessel. As the sphere made contact with the rectangular vessel the intersected geometry was calculated for flame volume and surface area. As the intersection with vessel increases, the shape of the flame would morph to resemble the walls of a cylinder.

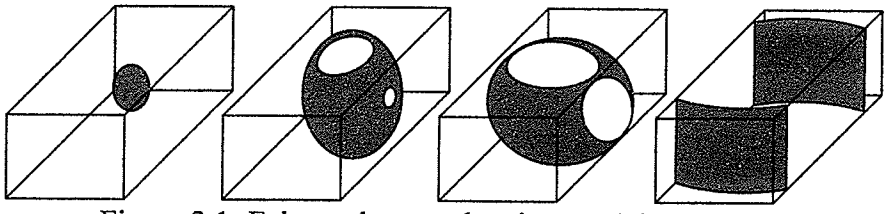

Figure 2.1: Fairweather combustion model [19]

Whitehouse et al [20] used an approach where the flame is a collection of triangles. At ignition, their flame begins as a small collection of adjacent triangles that form to create a small closed volume. Each triangle represents a surface that acts as a portion of the flame front. The enclosed volume is a representation of the burnt gas mass.

Propagation through the flame tracking is handled with vectors. For a specified time, a vector is generated as a perpendicular of the triangle from the previous time frame. The magnitude of the vector is the sum of the effects of diffusion, thermal expansion and the vent effects. This is determined for the specified direction and for the specified amount of time.

The simulation developed in their research uses theories that estimate the movement of the flame through flame advancement principles. The properties of the subsequent flame and burnt gas mass are used to estimate the overall pressure in the vessel.

Beyond the generalized geometric models, numerical models have been developed for deflagration simulation. Cummings et al [21] examined the ability of two codes to model both closed and vented deflagrations: Conchas-Spray and HECTR (Hydrogen Event Containment Transient Response). A simulated version of the LSVCTF was constructed be Lee et al [22] using the GOTHIC thermo hydraulic numerical package. Along with the LSVCTF, a long tube-like geometry and an arrangement using an obstruction were simulated to test the capabilities of GOTHIC for overall hydrogen simulation purposes. Sophisticated numerical packages, including CFD, have become common place in combustion analysis. For safety analysis, complex numerical analysis can be used to evaluate the distribution of combustible gases with in a volume [6, 23]. Otherwise they can be employed for direct combustion simulation [22, 24].

Venting guidelines [25, 26] have benefited from the application of complex numerical analysis. Despite their contributions, current venting guidelines continue to use the principles presented by Bradley [15], Swift [17] and Fairweather [19]. Continued development built up on the concepts introduced by these individuals should remain open. It is becomes easy to dismiss the effects of deflagration with the looming threat of detonation. Potential dangers within the deflagration phase must be highlighted since the maintenance of deflagration is considered a preventative device for avoiding detonation.

1.3. Objectives

The objective of this thesis is to provide continued development to the work of Bradley [15,16], Swift [17] and Fairweather [19].

- Reactive flame shape

  Previous work using geometric assumptions for flame shape, did not provide the opportunity for the flame to react to it environment, and were generally tied to a specific vessel geometry. The first goal is to stray away from these assumptions and allow each portion of flame to advance based on the immediate and unique surroundings.

- Pressure estimation

  The constructed simulation must provide an estimation of pressure throughout the duration of each run. Accuracy is not to be expected from these pressure profiles, but should demonstrate reasonable association to changes in hydrogen concentrations, vent size and ignition location.

- Visuals Representation

  Developing a visual component to the simulation is another goal. Bradley [16], Swift [17], Fairweather [19], and Mulpuru[10] generated effective models that were thoroughly documented in their geometric approach. Their models, however, did not provide a visual component. Providing visuals of the flame as it progresses presents an opportunity for the viewer to relate the production of pressure to the interaction of the flame with its containment.

- Exploration of web based distribution

  The operation and distribution of visual data will also be explored, by means of web based technologies.

Chapter 2:

Technical Background

2.1. Pressure Development

From Bradley et al [15], we find four formulae that will act as a basis for pressure calculation. The first examines the relationship between the rate at which the mass of burnt fuel accumulates as the flame advances and consumes unburnt fuel [15].

$$\frac{dm_b}{dt} = 4\pi^2 \rho_u S, \tag{2.1}$$

where m_b is the mass of burnt gas, ρ_u is the density of the burnt gas and S is the overall flame speed. Conversely, rate at which fuel is consumed is:

$$\frac{dm_u}{dt} = -4\pi^2 \rho_u S, \tag{2.2}$$

where m_u is the mass of unburnt gas [15]. The equation operates on the assumption that, again, the flame is spherical and that the gaseous fuel is uniformly distributed throughout the volume. Here, the rate at which fuel is consumed is a function of the local burning rate, S, and the gas density and the surface area of the flame front, in this case the surface of a sphere. This assumption lends itself to the volumetric rate of increase of the burnt gas:

$$S4\pi R^2 \frac{\rho_u}{\rho_b}, \tag{2.3}$$

where R is the radius of the burnt gas mass, assumed to be a sphere [15]. The density of burnt gas is denoted as ρ_b. A critical characteristic of this combustion system is a dynamic system that occurs causing the venting of gas from the system. As the flame front

advances, consuming fuel, the expansion of the burning flame against its unburnt surroundings cause as pressure growth, which is assumed to be uniform throughout the entire vessel.

While working the sub-sonic regime, the rate at which gas is vented is represented by:

$$\frac{dm_v}{dt} = C_d A_v \left\{ \frac{2\gamma p \rho}{(\gamma - 1)} \left(\frac{P_a}{P} \right)^{\frac{2}{\gamma}} \left[1 - \left(\frac{P_a}{P} \right)^{\frac{\gamma - 1}{\gamma}} \right] \right\}^{0.5}, \qquad (2.4)$$

where C_d is a vent discharge co-efficient, A_v is the vent area and ρ is the density of the venting gas or gases [15]. Specific heat ratio is denoted by γ, Pa is ambient pressure while P represents current total pressure. The values of specific heat ratio and density are dependant on the values associated with the gas exiting the system, whether burnt or unburnt. If a combination of both is leaving the system, then the total mass of vented gas becomes a ratio depending on the amount exiting.

The method to establish this experiment is that the vent remains covered till the pressure in the vessel becomes great enough to force the closed vent open. The case of vented combustion we are considering is specified in a different method. In the experimental setup examined here, the vent is opened at the onset of ignition. The effect of this is that the gaseous mixture is able to exit immediately after the beginning of the simulation. This significantly reduces the amount of fuel available to be consumed by the system. As the flame grows, the difference in ambient pressure outside the vessel and the overpressure within the vessel cause a greater amount of gas to be vented. An effect is demonstrated in Equation 2.4. This further reduces the amount of fuel available in the volume. This can effectively decrease the total energy stored in the initial mixture.

While vent effects can remedy a potentially dangerous situation by allowing fuel to escape from a combustible system, vent induced flows also increase the flame's burning rate. The increased interior pressure develops a flow through out the entire volume. This

cause flow field effects for both burnt and unburnt gases. As the vent flows affect the gas within the flame and surrounding it the flame is allowed to stretch and distort, increasing the overall area and thus the burning rate.

When moving away from the spherical assumption, Equation 2.1 can be generalized to accommodate all other surface shapes [11].

$$\frac{dm_b}{dt} = \rho_u \oint S_t dA\,, \tag{2.5}$$

where S_t is laminar burning velocity. Again, the rate of increase of burnt mass is associated with the current surface area. In this form, simulation can accommodate the variety of deformation caused by the vent induced flows.

In accordance to the conservation of mass we have:

$$m_u + m_b = m_\tau - m_{uv} - m_{bv}\,. \tag{2.6}$$

Again, m_b is the mass of burnt gas and m_u is the mass if unburt gas. The total gas mass is m_τ, while m_{uv} and m_{bv} denote the mass vented unburnt and burnt gases respectively. The current mass of burnt and unburnt gas within the volume is equivalent to the difference between the total mass and the combined mass of the vented gas. Through this relationship we are able to derive the rate equation for pressure [15].

$$\frac{dP}{dt} = \left[\left(\frac{\rho_u}{\rho_b} - 1\right)\oint S_t dA - \frac{1}{\rho_b}\frac{dm_{vb}}{dt} - \frac{1}{\rho_u}\frac{dm_{vu}}{dt}\right]\frac{P}{\left[V_b\left(\frac{1}{\gamma_b} - \frac{1}{\gamma_u}\right) + \frac{V_o}{\gamma_u}\right]}, \tag{2.7}$$

where, V_o is the total volume, and the V_b is the burnt gas volume. From this relationship the current pressure within the volume can be found, while accounting for the effects of vented gases, whether they are burnt or unburnt.

2.2 Flame advancement

With established formulas for determining the properties required from the vented combustion system. A method for advancing the flame is necessary to satisfy the requirements for the flames surface area. Equation 3.8 was introduced by Whitehouse et al [10].

By considering a position on the advancing flame surface, it can be said that the advancement of the flame is approximated by the formula:

$$\frac{d\vec{R}}{dt} = \vec{S_t} + \vec{S_t}\left(\frac{\rho_u}{\rho_b} - 1\right)W + \vec{S_v}, \qquad (2.8)$$

Where $\vec{R}$ is the traveling distance of the flame in a specified direction. Laminar burning velocity is also represented by $\vec{S_t}$. W represents a thermal expansion value, while $\vec{S_v}$ indicates the burning velocity affected by the vent. Equation 2.8 represents the rate at which that position on the flame front will advance for a given point in time. This equation can be further broken down into its 3 parts.

The first component is diffusion. Diffusion is of a constant magnitude, representing the consumption of the combustible mixture. In a single direction, it represents the steady expansion of the flame front till the encounter of an obstacle. In two-dimensions, its development takes shape in the form of a circle with an advancing perimeter. In 3D, a sphere develops with a steadily increasing radius.

The second component is thermal expansion. As fuel is consumed the accumulated mass of burnt gas is hot relative to its surrounding on unburnt gas. Like all hot gas masses, the tendency is to expand. This is the main principle governing this component of the flame

tracking mechanism. The amount a flame will advance via thermal expansion is dependant of the amount of space available ahead of the flame. If there is an abundance of space available, expansion will increase. However, as a flame front approaches an obstacle or a wall, the confinement reduces thermal expansion, as the surrounding gases ability to compress is lost in small spaces.

The final component of the flame tracking model is the vent induced flow. The main mechanism causing this advancement is the pressure difference between the interior combustion system and the exterior, which is assumed to be atmospheric. What this produces is a suction effect of all the gases within the vessel. The degree of suction on a specific portion of gas, is dependant on its proximity to the vent. This is true for the advancing flame front. The consequence of the vent induced flow is the deformation of the flame towards the vent, increasing the surface area and overall burning rate. The application of these principles in combination with the relationship was discussed in the previous section, which acts as the foundation for the presented simulation.

Chapter 3:

Simulation Methodology

The combustion simulation will take on a finite volume approach. Examinations of the mechanics within a single cell and the interactions of multiple cells are required.

A simulation volume is considered a closed volume, filled with unburnt combustible fuel. Therefore each cell will begin as a finite volume of unburnt gas. As burnt gases are consumed, cells will carry burnt gas. The collection of cells holding burnt gas will represent the propagation of the flame. Activity only occurs where cells are transitioning from unburnt to burnt cells. This represents the propagating flame front. The process is iterative with a user defined time step.

3.1. Inter-Cellular Mechanics

Burning in a single cell occurs in a single direction. This will follow the x, y or z axis, in either the positive or negative direction. As the flame enters a cell it is considered active. When a cell becomes active, the burning direction is established (as described in the following section).

Activity in a cell is denoted by a percentage. This percentage denotes how far the flame has traveled in that cell, in that particular direction. Assuming, that they travel uniformly over the cross-section of the flame, this value also denotes the percentage of burnt gas consuming the cell. Once the value of activity reaches one hundred percent, the cell represents a volume of burnt gases. The simulation is designed in such a way that a cell will take a number of iterations to completely fill up with burnt gases. It cannot become active and be considered completely burnt within one time iteration. Completely burnt cells are no longer considered active, but maintain their hundred percent values.

While the cell is active, an iterative process occurs to simulate the movement of the flame front within the cell. Movement within a cell only occurs in the assigned direction. As stated in Equation 2.8, the magnitude of the movement will be calculated based on the effects of diffusion, thermal expansion and vent effects. Diffusion is a constant that is a defined value for the simulation.

The process for determining the propagation by thermal expansion, begins by first establishing the amount of space available ahead of the flame. With the defined direction, the cell calculates the distance from its position to the nearest obstacle or boundary. This association is then used to ascertain the flame's traveling distance by expansion within that time frame.

Vent induced flows are solved as part of the process used for determining thermal expansion. While defining the distance between a cell and a constraint, if the opening is found ahead of the flame then vent effects be considered. First, thermal expansion is set at the maximum value, as if there is no constraint. Ideally, the vent induced flow is solved as a function of distance from the vent and the vent dimensions. These three properties are then combined to give the total intercellular flame movement for that iteration.

3.2. Multi-Cell Interaction

For the burnt gas mass to grow, the flame must be extended into adjacent cells. The propagation method through multiple cells is considered a burning zone concept. The burn percentages of all active cells adjacent to an inactive cell are considered. Their values are weighted and summed. The weight of an adjacent cell sharing a face is higher then the weighted of a cell sharing an edge, or a vertex. For Figure 3.1, when considering the possible activity of cell A, the weight of the activity for cell B is greater than that of cell C. If the total of the weighted burn percentages is equally to a pre-defined critical value, then the inactive cell in question becomes active (Figure 3.2). The burning direction of the cell is defined as the perpendicular to the shared face of the adjacent cell providing the largest burn percentage.

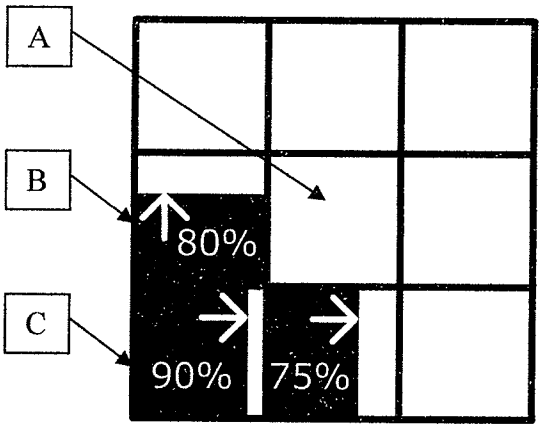

Figure 3.1: Burning Zone Adjacent Cell Weights

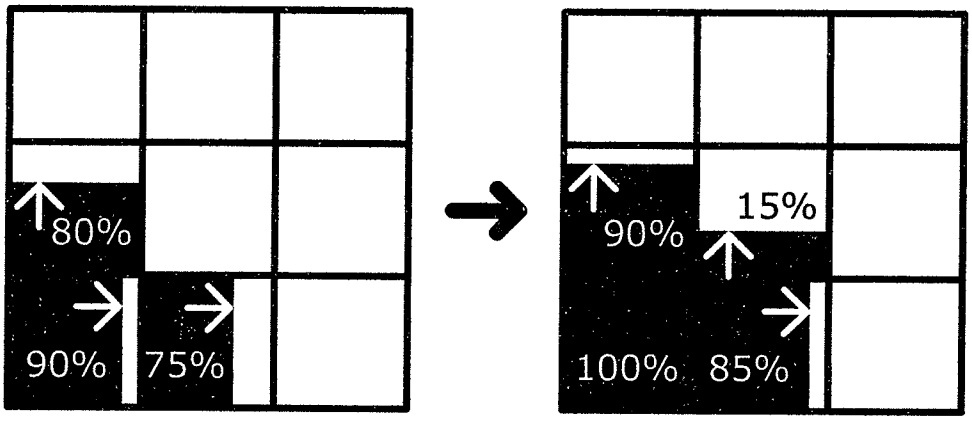

Figure 3.2: Burning Zone Propagation

A simultaneous system for multi-cellular behavior was triggered when a cell's activity reaches one hundred percent. Within this condition, it is assumed that the cell is completely filled with burnt gas and that the flame must move on beyond this cell. If an active cell reaches a complete burn all inactive face sharing cells will be activated (Figure 3.3). This is done regardless of the cumulated of burn percentages of the adjacent cells. The burn direction for the cell is defined as the cell becomes active. This is the

perpendicular to the shared face. When all cells are completely burnt, the propagation will end.

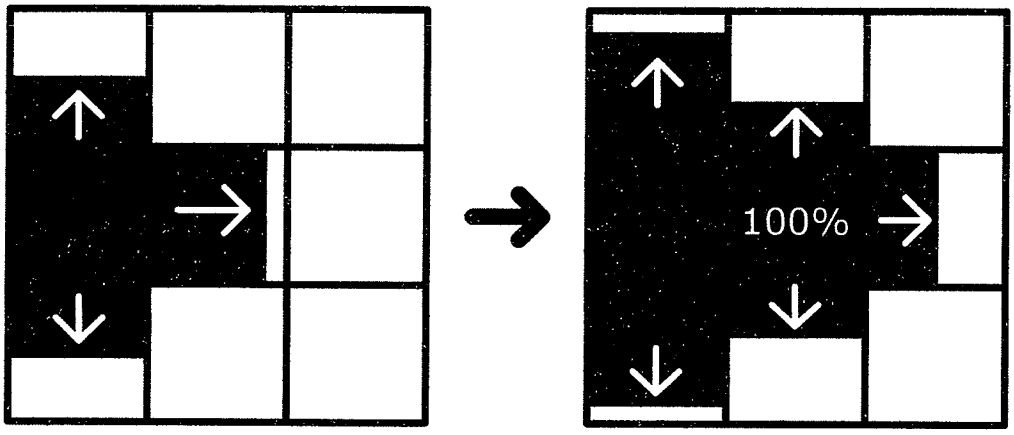

Figure 3.3: Full Burn Model

3.3. Pressure Estimation

The development of pressure is directly related to the surface area of the flame front and the collected mass of burnt gases. Equations 2.1, 2.2 and 2.3 were built under the assumption that the flame front advanced in a spherical pattern. That assumption does not hold true here, with an expected irregular flame shape, the more general Equation 2.5 is more relevant. Values for flame front surface area and volume are acquired from the cellular flame propagation governed by the flame advancement formula, Equation 2.8.

Burnt gas mass is obtained from the accumulation of burnt gas cells. Completely burnt cells are taken as total cell volume. Active cells are accumulated as a percentage of the entire cell. This is based on the direction and the calculated propagation of the flame within the cell. For a single cell, surface area is taken as the area of the perpendicular face from the established burn direction. Overall surface area is the accumulation from each active cell.

With these values, the solution for the change in pressure at any instance is given by Equation 2.7 [15]. With respect to the iterative process, Equation 2.7 lends itself to:

$$\frac{\Delta P_{(n)}}{dt} = \left[\left(\frac{\rho_u}{\rho_b} - 1\right) S_t t A_{(n)} - \frac{1}{\rho_b}\frac{\Delta m_{vb(n-1)}}{dt} - \frac{1}{\rho_u}\frac{\Delta m_{vu(n-1)}}{dt}\right] \frac{P_{(n-1)}}{\left[V_{b(n)}\left(\frac{1}{\gamma_b} - \frac{1}{\gamma_u}\right) + \frac{V_o}{\gamma_u}\right]}, \qquad (3.1).$$

For the current time frame, current values for surface area and volume are used in combination with values of total pressure and venting from the previous time step.

The mass of gas vented from the system is solved by Equation 2.4 [15]. This equation can be applied to burnt or unburnt gases by substituting properties for either. By iteration, the amount of gas leaving for a time step for unburnt and burnt gases, respectively, are:

$$\frac{\Delta m_{vu(n)}}{dt} = C_d A_v \left\{ \frac{2\gamma_u P_{(n-1)} \rho_u}{(\gamma_u - 1)} \left(\frac{P_a}{P_{(n-1)}}\right)^{\frac{2}{\gamma_u}} \left[1 - \left(\frac{P_a}{P_{(n-1)}}\right)^{\frac{\gamma_u - 1}{\gamma_u}}\right] \right\}^{0.5} t, \qquad (3.2)$$

$$\frac{\Delta m_{vb(n)}}{dt} = C_d A_v \left\{ \frac{2\gamma_b P_{(n-1)} \rho_b}{(\gamma_b - 1)} \left(\frac{P_a}{P_{(n-1)}}\right)^{\frac{2}{\gamma_b}} \left[1 - \left(\frac{P_a}{P_{(n-1)}}\right)^{\frac{\gamma_b - 1}{\gamma_b}}\right] \right\}^{0.5} t, \qquad (3.3).$$

Both equations remain true in the subsonic regime (which is assumed true), and when $P > P_a$. Initial set up considers that the exiting gas is either burnt gas or unburnt gas. The transition occurs when the flame reaches the vent. Prior to this event only unburnt gas is vented. Later simulations considered a combination. In these cases, the ratio of burnt and unburnt gas is equal to the ratio within the volume.

3.4. Assumptions

Assumptions made during the development of the simulation model include:

- Initial conditions are assumed that the vessel is completely closed. The vent opening is covered.
- At the moment of ignition the vent will open fully. The cover will blow away from the vessel leaving no effects on the exiting gas flow.
- The gas mixture will fill the volume and assumed uniformly distributed at the start. The flame propagates until the entire defined volume of fuel is used. At the end of a simulation run the volume is completely filled with burnt gas.
- Pressure at any given time is uniform through the entire vessel.
- The ratio of vented burnt to vented unburnt gas is equivalent to the ratio of burnt to unburnt gas within the volume at any particular time.

All volumes are defined as rectangular with uniform cell dimensions along each axis. All outer cells are defined as boundaries, flame growth is limited to these extent. Vents are defined as a portion of these boundaries. Other predefined shapes (i.e. spheres, cylinders) are created by setting boundaries within the outer extents. Gas mixture is assumed uniformly distributed through all cells not defined as boundaries or vents.

3.5. Simulation Structure

The simulation processes are shown in Figure 3.4. At the beginning of each run the burn parameters, test volume dimensions, boundaries, vent location and size and ignition point are established, based on user specifications. Simulation duration is based on the defined time step and total time.

The recurring loop begins with the search for active cells representing the flame front. Once ascertained, the distance to a boundary is solved using the cells specified burn direction. At this time relation of a flame front cell to the vent is also determined. With

this information it is possible to solve for the traveling distance of the flame. The flame is the propagated within the active cells. Once the flame completely crosses a cell the cell is considered fully burnt and the search for active cells will by pass the location.

At each interval, after the flame has been propagated, the values for the flame surface area and burnt gas volume is collected. The volume ratio of burnt gas to unburnt gas is calculated. This data from the burn is then used to solve for the pressure rise from Equation 3.1, and the mass of burnt gas and unburnt gas are leaving the system based on Equations 3.2 and 3.3.

At this point the simulation will loop to the next time step. Cells on the flame front will be identified and the sequence of steps will be repeated. This will continue until the established time is reached. Output data for graphing of physical properties, including pressure and surface area, is created as the code progress through each time step (Figure 3.5). Data to be used for graphics either through Tecplot or VRML (Chapter 5) are also created as the code progress, but not at every time step.

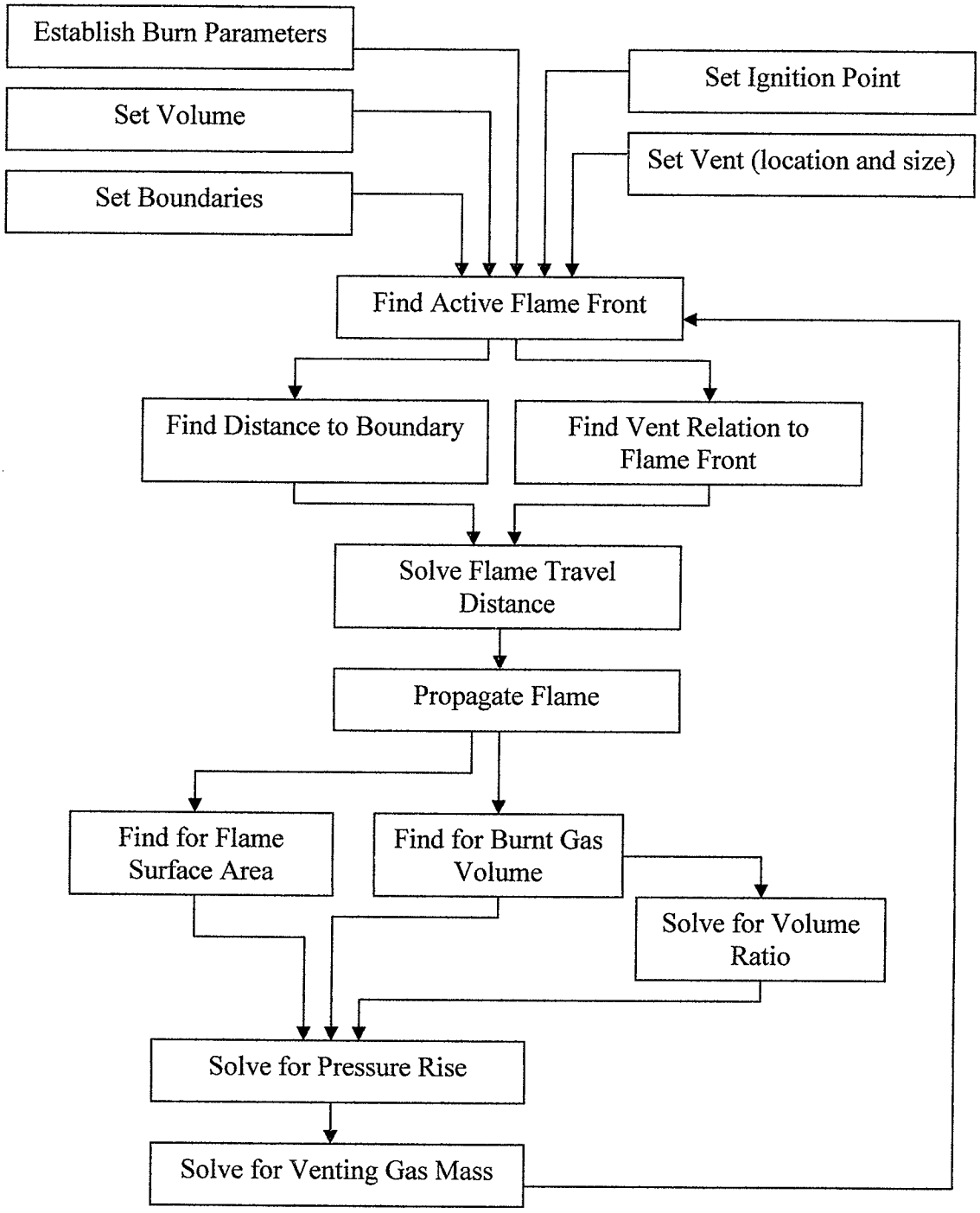

Figure 3.4: Simulation Structure

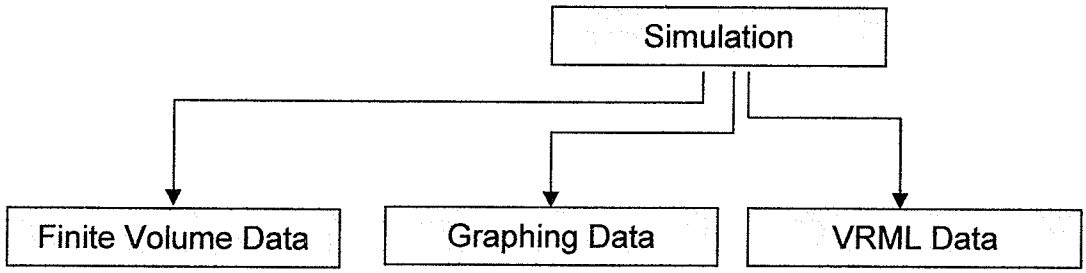

Figure 3.5: Simulation Data Output

3.6. Model Development

The initial proposal for this research was focused mainly on the graphical development of a propagating flame in a vented volume. The flame tracking model was the core of code. Early builds had the flame traveling over multiple cells in one time step, and included considerations for obstacles and a simple vent flow model. The methods developed in the early code were intended for eventual use directly into VRML, to develop a complete web-based solution. The methods developed would eventually be considered for applications to a real-time simulation.

Subsequently, the addition of the estimating pressure generation was added as an objective. When the principles for pressure estimation were applied to the existing code, the results were unusable. It was decided that the nature of the graphical simulation was in compatible with the new objectives. A number of changes were made at this point. The most significant was the addition of physical properties relating to the pressure generation. The iterative process was refined. The early graphic-based design considered 10 to 20 frames of animation, now anywhere from 2000 to 7000 time iterations would be required. Flame movement could no longer exceed a cell length in a single iteration. The code would now produce large data files, and run time magnitudes are increased to minutes rather than seconds. Web implementation would have to be removed for later re-evaluation. The modified code removed obstacles, to properly test the relationships governing pressure generation. A simple vent effect model was considered, which was involved the addition of a predefined value.

Accuracy was not tested, but rather general behavior. The tests for pressure had proved positive for general behavior. Tecplot visual generation saw further development, and VRML concepts were reintroduced in a limited role. The concern was over the shape of the flame. The simulation used a multi-cell propagation technique as demonstrated by Figure 3.3. Using this method led to a prismatic, diamond shaped graphical growth. A number of ideas were applied and tested with limited success. Eventually the burning zone concept was employed. This method helped to "round out" the shape of the flame. In the new approach, the major concern was the use of the existing vent effect concept. As venting concepts were considered, a model tied to thermal expansion would be used in the interim.

Chapter 4:

Simulation Results

4.1. Testing Scenario

Results from the simulation are compared with the data from multiple sources. All hydrogen burning velocities are estimated based on the results from Koroll et al [27] unless values are specified in the research of the following authors.

4.1.1. LSVCTF

One arrangement was based on the former LSVCTF [11]. The large scale experiments were conducted in a 4m x 3m x 10m volume with venting at one end of the 10 m length (Figure 4.1). Ignition location as well as vent sizings were adjustable.

Data from Lee et al [22], comparing GOTHIC test data to actual simulation results, will be used for comparison. The suggested experiment encompassed the entire volume with a central ignition. A hydrogen concentration of 14.2% was used with a rectangular vent size of $1.12m^2$.

Sitar et al [11] recorded preliminary test data at the LSVCTF. The test specified the use of the entire volume, along with multiple vent sizings and hydrogen concentrations. Central ignition points were used in all cases. These tests include 8.5% and 9.0% with a vent size of $1.12m^2$ and 11% hydrogen with a $0.56m^2$.

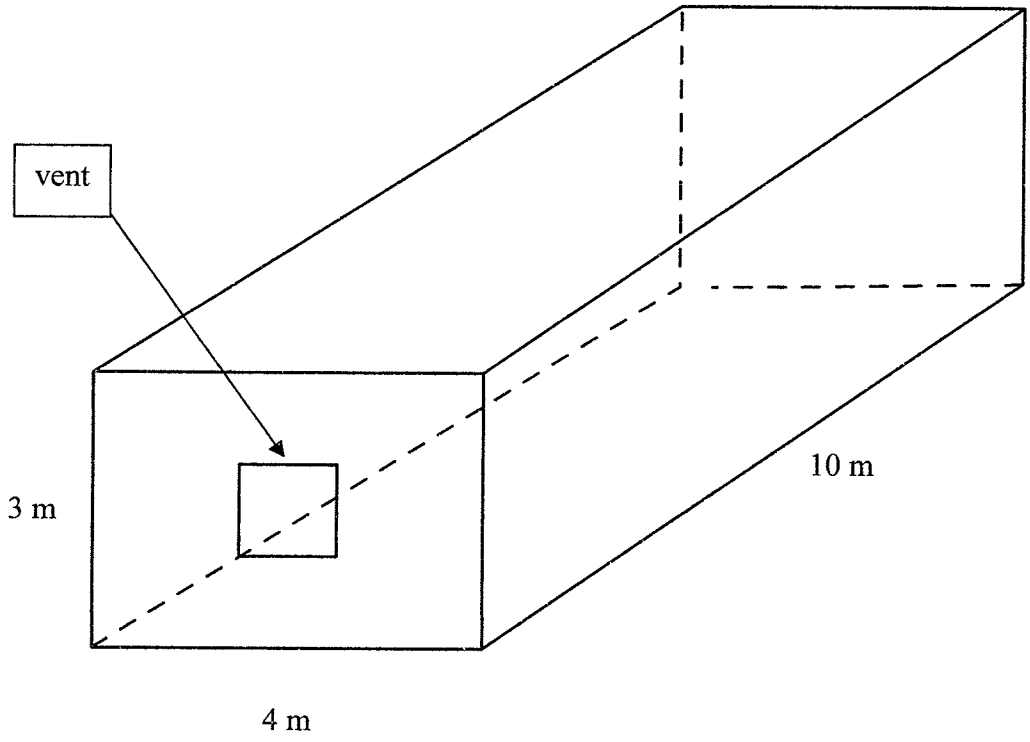

Figure 4.1: LSVCTF volume

4.1.2. Cummings (HECTR and Conchas-Spray)

The motivation behind the research of Cummings et al [21] was to consider the role that simulation could play in nuclear safety research through the examination of HECTR and Conchas-Spray. Cummings et al [21] considered a cylinder arrangement in the use of the HECTR and CONCHAS-SPRAY codes. Testing was conducted with and without obstacles. The data from the volume without obstacles are considered. The cylinder is measured 4.88m in length, 1.22m diameter, and a 0.86m diameter vent. Tests were conducted at 15% and 30% hydrogen.

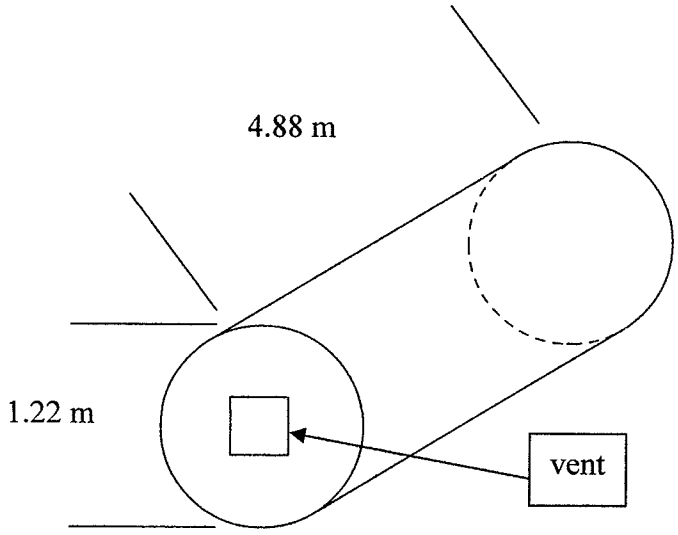

Figure 4.2: Cummings volume

4.2 Results and Discussion

4.2.1. LSVCTF

The model was run using a mock up of the LSVCTF. The volume was specified at 10m x 4m x 3m along the x, y and z axis respectively. Cells were defined at 45, 40 and 40 cells, again along the x, y and z axis respectively, measuring 0.22m x 0.1m x .075m. The outer cells were designated at boundaries, reducing the overall dimensions by one cell on each side. Vent cells were designated at one end of the 10m length and centered accordingly. Initial tests considered central ignition.

LSVCTF Preliminary Test Data Comparison

The initial simulation run involved the $1.12m^2$ vent size at 11% hydrogen. The comparison data from the Sitar et al [11] is provided in Figure 4.3. The pressure profile generated by the test is presented in Figure 4.4. Figures 4.5 and 4.6 represents the surface area and volume of the burn area. Graphical representation is provided in Figure 4.7.

Peak pressure is recorded at 113317 Pa. This provides an overpressure of 11.99 kPA. Overpressure values suggested by the Sitar et al [11] are approximately 45 kPa. Overall burn time is 16 seconds from the point of ignition. The active region of the Sitar et al [13] suggests nearly 9 seconds of burn activity.

The results significantly deviate from the test data produced at the LSVCTF [11]. A lack of proper vent effects is the likely cause of this difference. Improved vent effects would have increased the rate of burning towards the vent. This would have increase the overall surface are of the flame leading to higher pressure values as well as faster burn times.

The relationship between the flame surface area and pressure is clearly identified in Figures 4.4 and 4.5. Here peak pressure coincides with maximum surface area for the flame. The maximum rate of volume increase also exists in the same region of time. In terms of deflagration, these findings reinforce that the rises in pressure increase with increases in available burning area. As the opportunity to consume fuel escalates, so does the volume of burnt gases, leading to the rise of expansion forces within the volume.

The flame shown in Figure 4.7 demonstrates the increase in volume of the burnt gas mass. The vent is at the center of the lower left hand surface. Its surface represents the propagating flame front.

The flame front advances further in the directions where it is given the most room to expand. By the frame at 6 seconds it is clear that the flame grows most along the x axis. Conversely, propagation appears hindered in the y and z directions, where the flame is given the less space to expand. The result is a pronounced ellipsoid shape favoring the volumes longest direction.

In each successive time step it is clear that the surface area is increasing. The peak pressure is reached at approximately 9 seconds. At this point it can be seen that the flame approaches the maximum size available within the volume, even with the quenching around the vent. By 10 seconds the burnt gas mass has begun to make contact with the

volume wall. This effectively quenches the propagating flame in those spaces, reducing the flame front and mechanism for producing expansion forces. Overall pressure is reduced.

The frame at 8 seconds begins to show an increase in flame front propagation towards the vent, as opposed to the opposite end, which is facing a wall. The increase towards the vent is distinguishable, but not overly distinct. This suggests that the proposed venting mechanism is lacking. In this case the vent effects are set as the maximum rate of thermal expansion available for the burnt gas against the surrounding unburnt gases. The lacking effects of the vent on the growth of the flame surely caused a reduction in the pressure produced.

The other preliminary tests for the LSVCTF included data for $0.56m^2$ sized vent at both 8.5% and 9.0% hydrogen. The data from both vary significantly. The test at 8.5% remains active for an entire minute, with a peak over pressure at approximately 1.3 kPa. The test at 9% burned in less than 12 seconds and achieved a maximum 13kPa overpressure.

The model was run with a flame speed of 0.05m/s to simulate burning in this region of hydrogen concentration. The results lead to a burn time of over two minutes and a peak pressure or 2.39 kPa. While these values appear to be similar in magnitude to that of the 8.5% burn conducted by Sitar et al [11], comparison to both sets of data continue to suggest that the simulation of vent effects need to be improved.

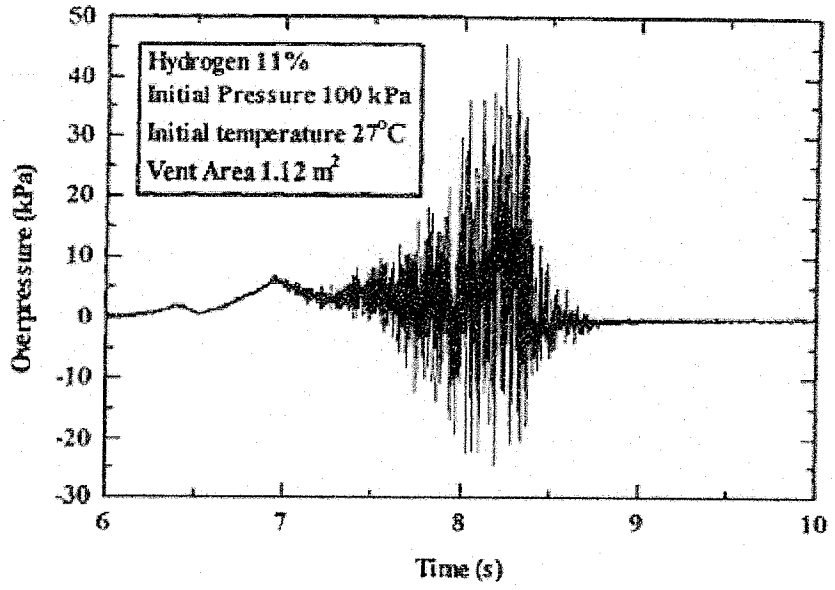

Figure 4.3: Pressure profile. LSVCTF preliminary [11]

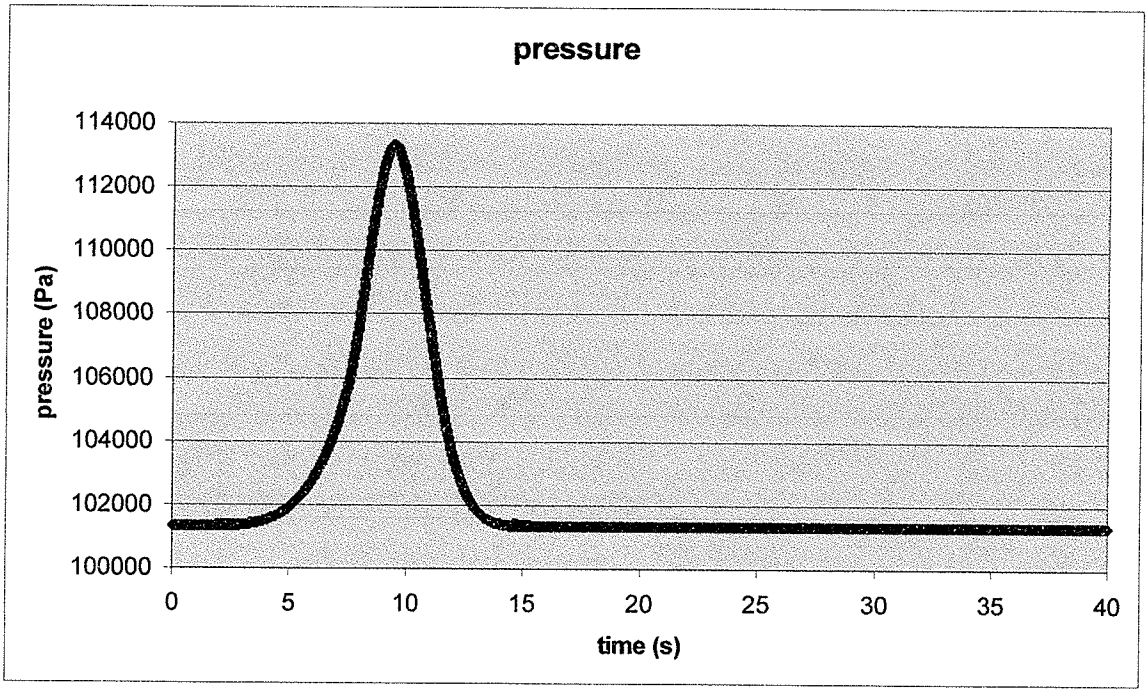

Figure 4.4. Pressure Profile. Test 10m x 4m x 3m volume. Vent size 1.05m x 1.05 m. Hydrogen concentration 11%, flame speed 0.4m/s. (simulating Sitar[11])

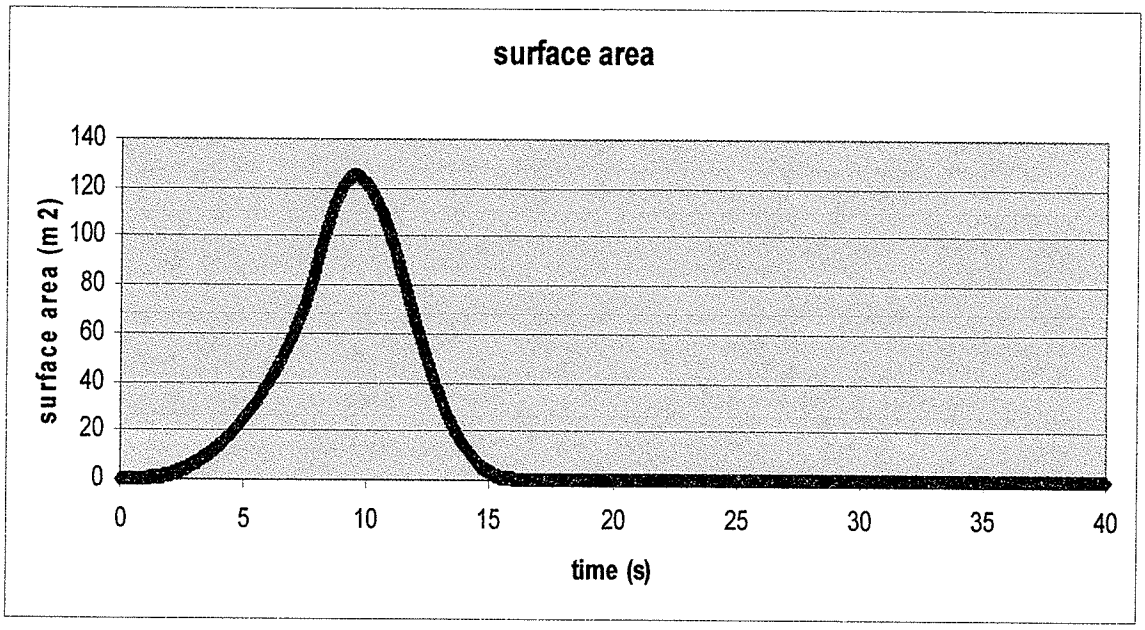

Figure 4.5. Surface Area. Test 10m x 4m x 3m volume. Vent size 1.05m x 1.05 m. Hydrogen concentration 11%, flame speed 0.4m/s. (simulating Sitar[11])

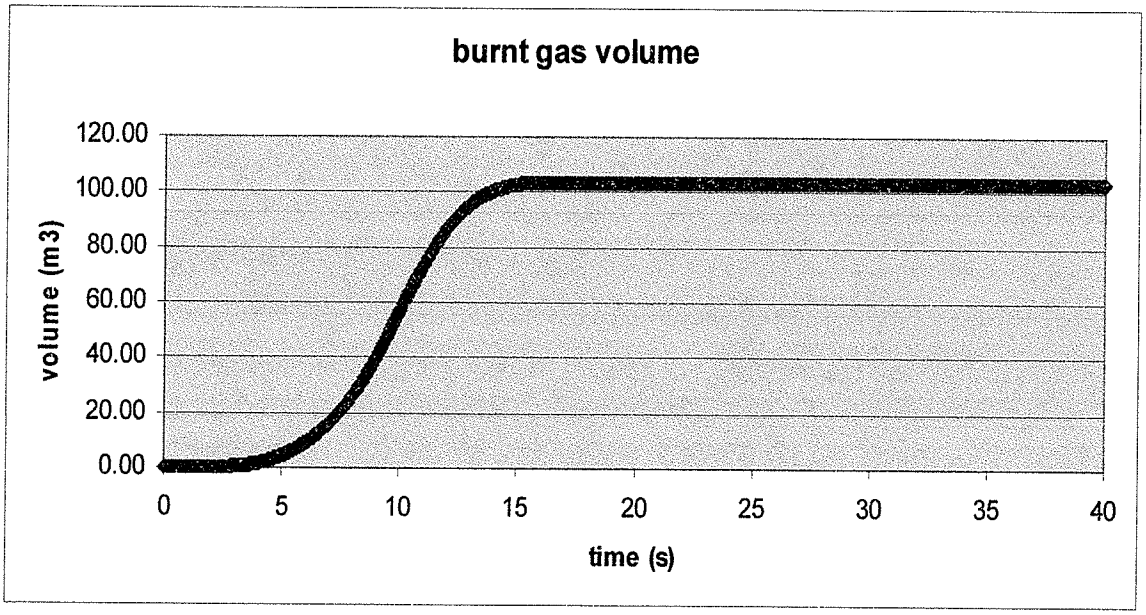

Figure 4.6. Burnt Gas Volume. Test 10m x 4m x 3m volume. Vent size 1.05m x 1.05 m. Hydrogen concentration 11%, flame speed 0.4m/s. (simulating Sitar[11])

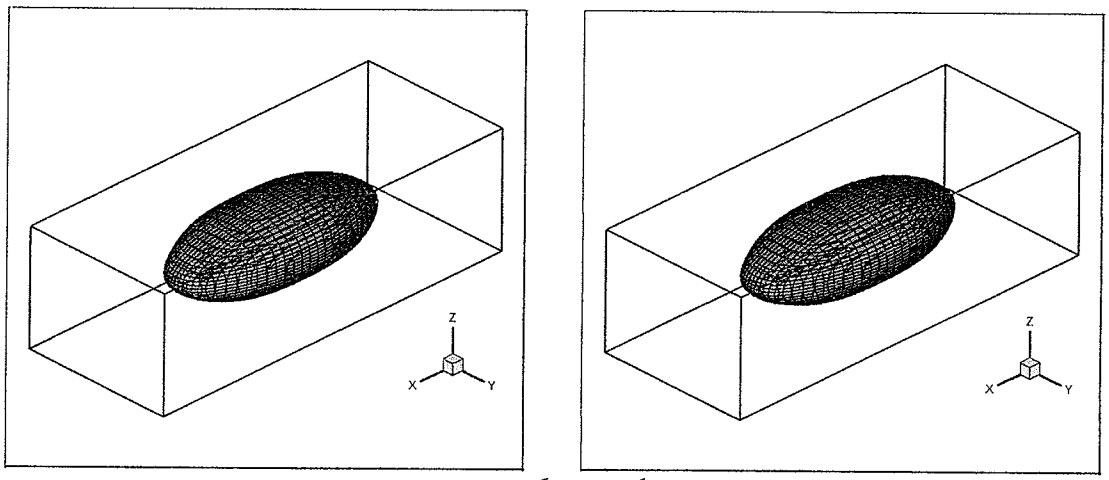

t= 6 seconds

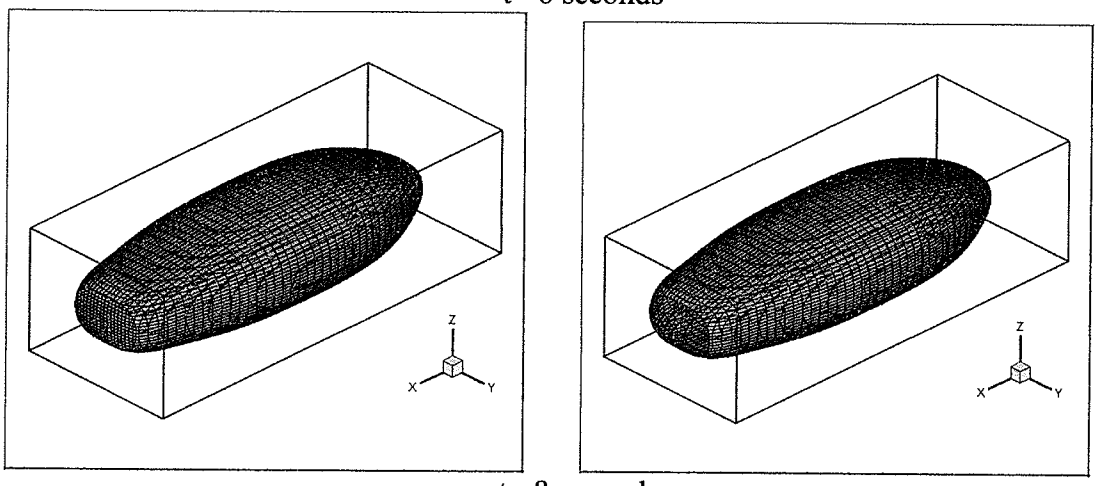

t= 8 seconds

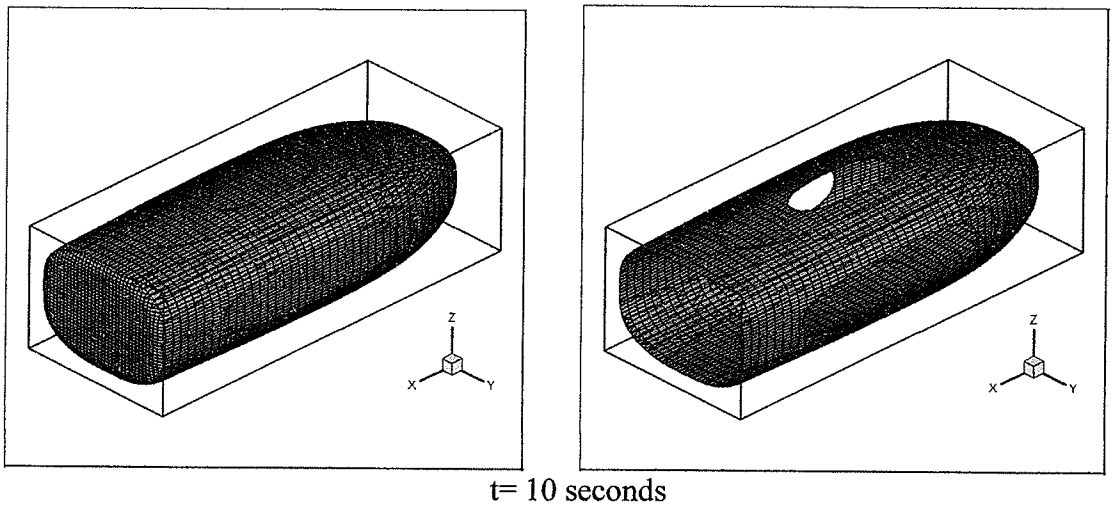

t= 10 seconds

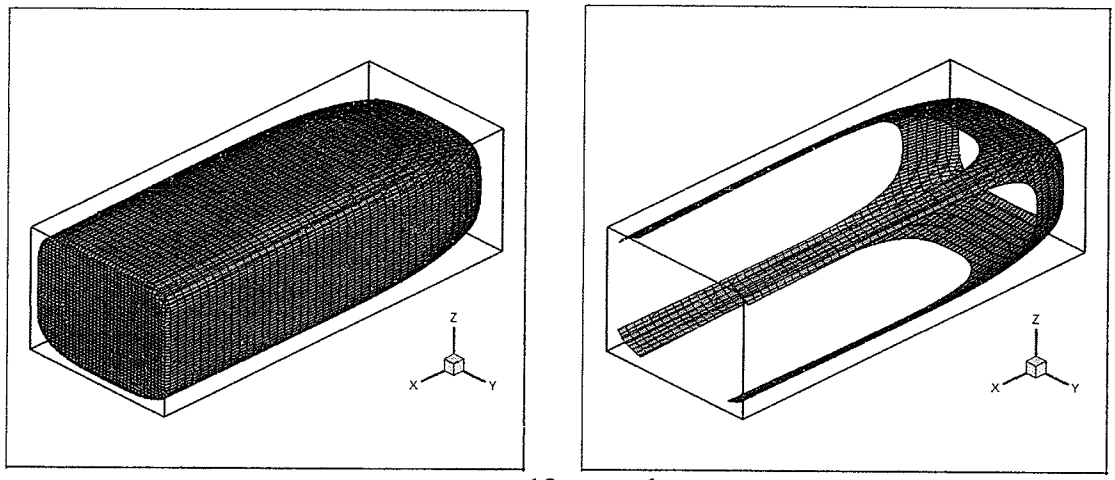

t= 12 seconds

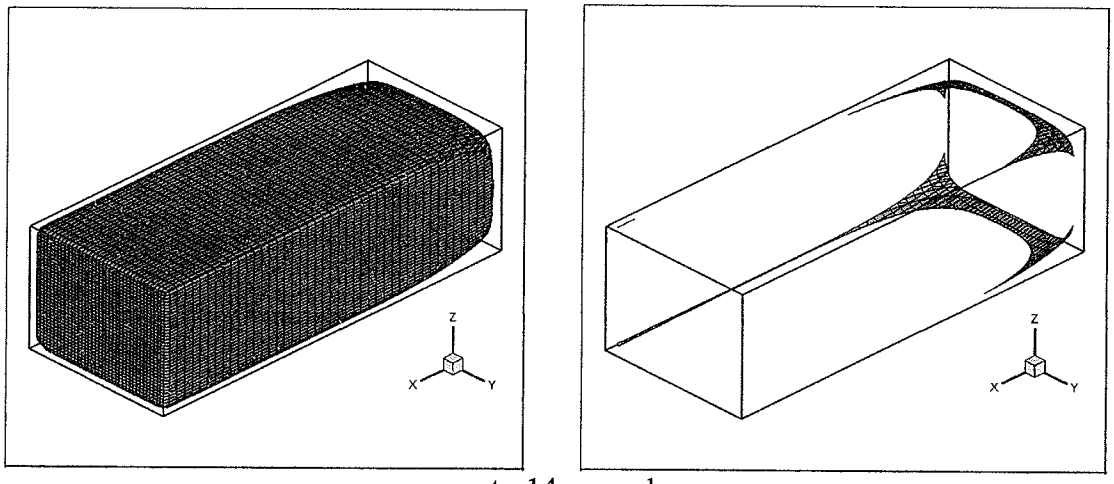

t= 14 seconds

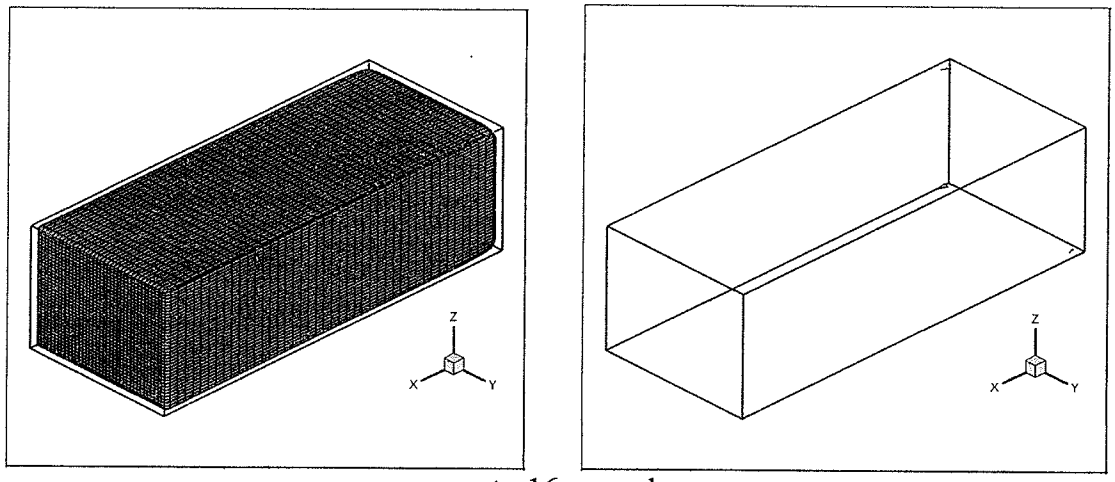

t= 16 seconds

Figure 4.7. Flame Representation. Test 10m x 4m x 3m volume. Vent size 1.05m x 1.05m. Hydrogen concentration 11%, flame speed 0.4m/s. Burnt gas volume (left), flame surface area (right) (simulating Sitar[11])

GOTHIC Simulation

The pressure profile created by Lee et al [22] is presented in Figure 4.8. The pressure profile for the run simulating the work of Lee et al [22] is presented in Figure 4.9. Figures 4.10 and 4.11 represent the surface area and burn volume, respectively. The flame is visually represented in Figure 4.10. Peak pressure is 144546 Pa or an overpressure of 43.22 kPA. Overpressure values suggested by the Lee et al [22] are approximately 38 kPa. The overall burn time is 8 seconds, as opposed to the less than 4 seconds of activity suggested by Lee et al [22].

The resulting peak pressure for this test is much closer to the values collected by Lee et al [22]. In comparison to the run simulating Sitar et al [11], the higher rates of increase in both surface area and volume led to the increased pressure values. In this instance the increased rate of fuel consumption, increases the rate of volume increase and the expansion forces produced by the burnt gas volume. Visually this can be seen when comparing Figure 4.11 to Figure 4.6. Peak pressure is achieved at approximately 5 seconds in Figure 4.9. In Figure 4.12, frames at 4 and 6 seconds exemplify the peak surface area and the beginning of quenching for the flame front. The flame is able to reach maximum surface area, which is reduced with contact to the wall.

The same venting principles are used from the previous test. The difference in burn time continues to suggest the lack of proper vent effects. Accelerated propagation from the vent would only increase the peak pressure. The higher flame speed of this test from the previous test would lead to a reduced effect in pressure increase in comparison.

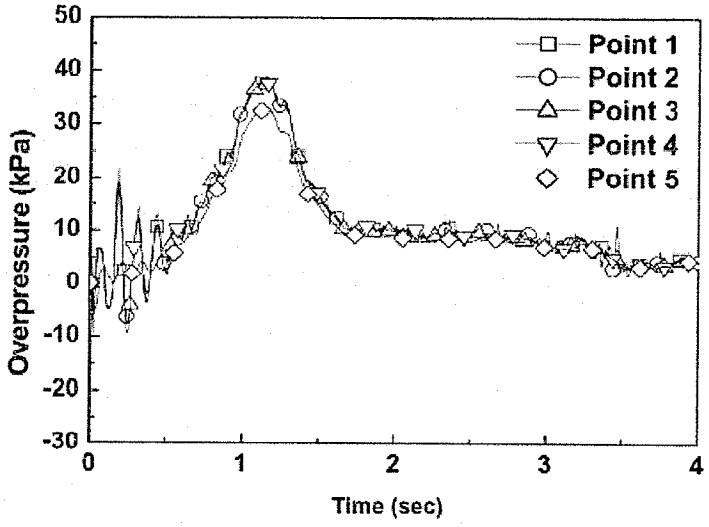

Figure 4.8: Pressure profile. Lee [22]

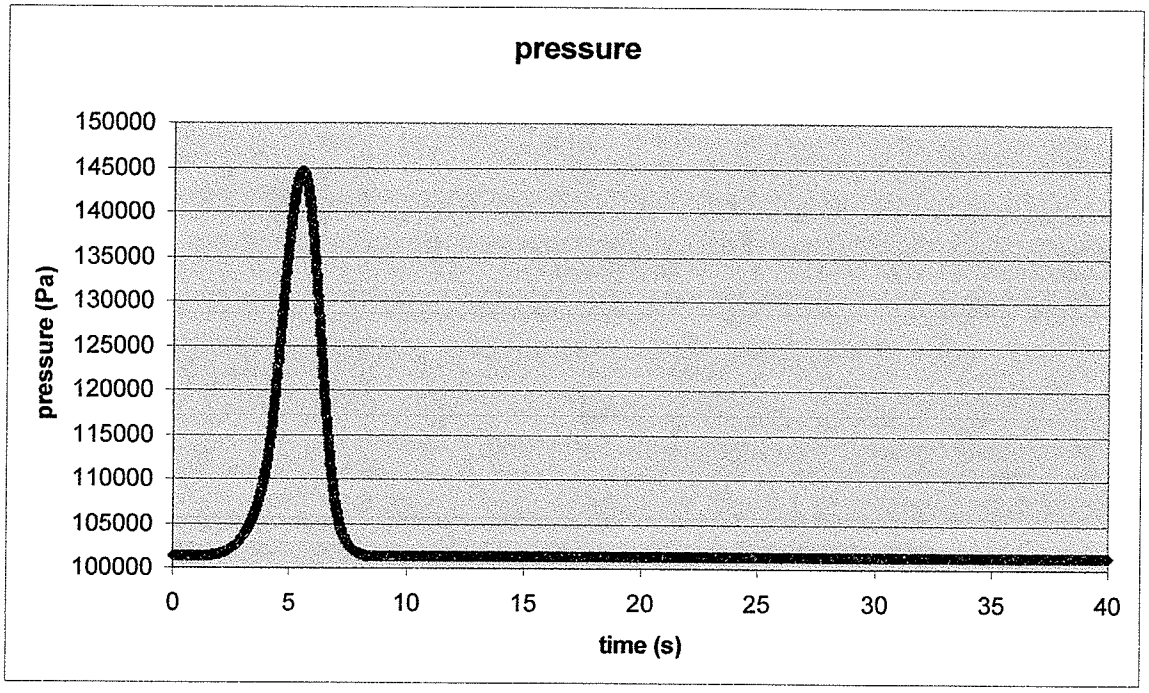

Figure 4.9. Pressure Profile. Test 10m x 4m x 3m volume. Vent size 1.05m x 1.05 m. Hydrogen concentration 14.2%, flame speed 0.7m/s. (simulating Lee[22])

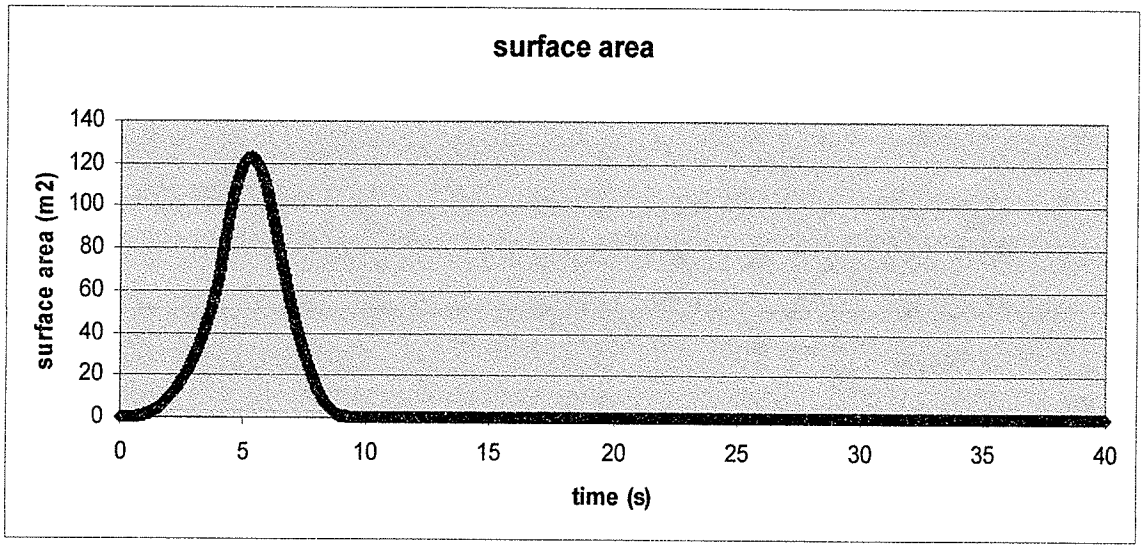

Figure 4.10. Surface Area. Test 10m x 4m x 3m volume. Vent size 1.05m x 1.05 m. Hydrogen concentration 14.2%, flame speed 0.7m/s. (simulating Lee[22])

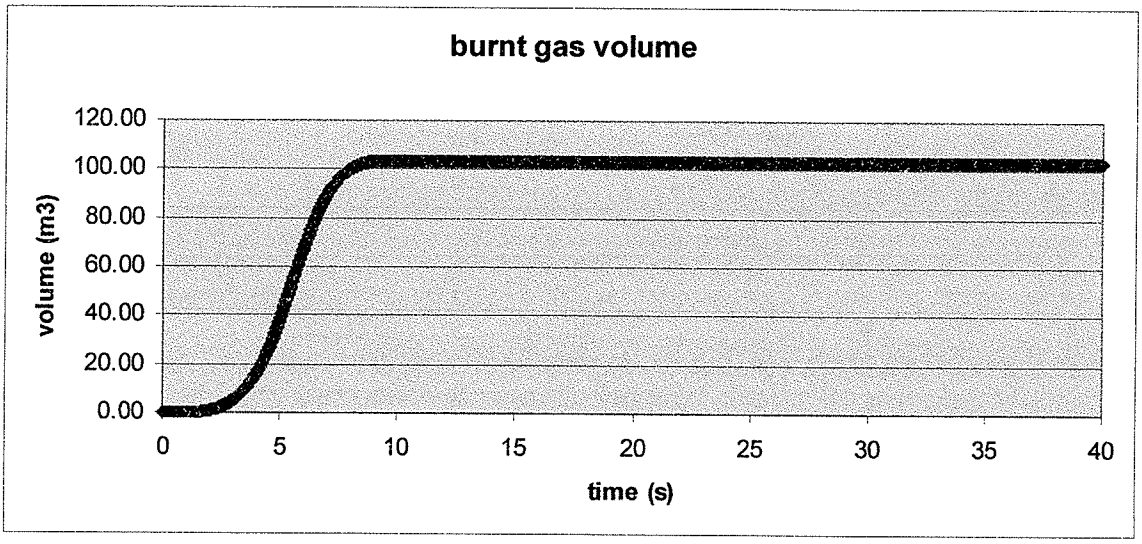

Figure 4.11. Burnt Gas Volume. Test 10m x 4m x 3m volume. Vent size 1.05m x 1.05 m. Hydrogen concentration 14.2%, flame speed 0.7m/s. (simulating Lee[22])

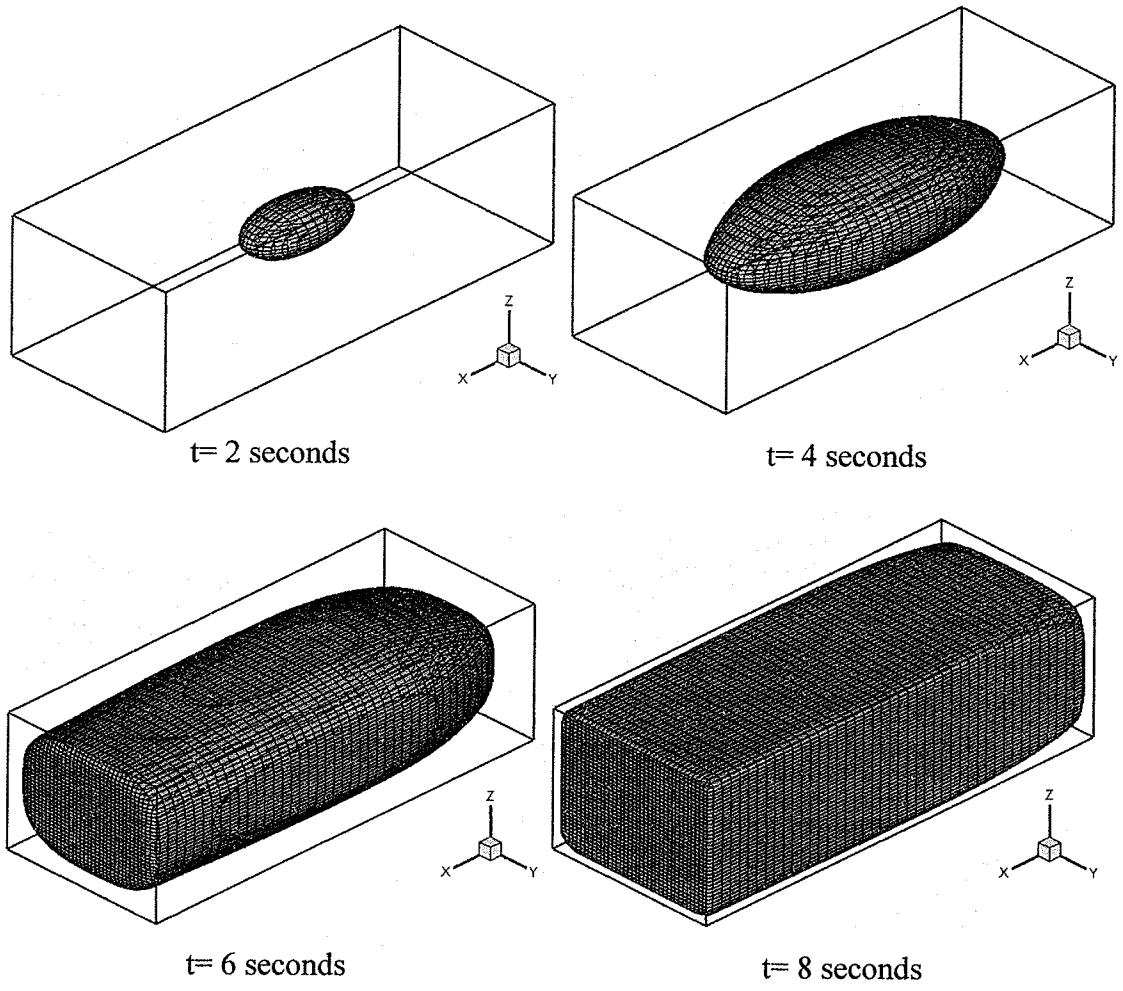

Figure 4.12. Flame Representation. Test 10m x 4m x 3m volume. Vent size 1.05m x 1.05m. Hydrogen concentration 11%, flame speed 0.7m/s. (simulating Lee[22])

LSVCTF Vent Size Analysis

It has been proven that the peak pressure recorded for the simulation run representing the preliminary run by Sitar et al [11] is lower than the expected value. Even with the lack of accuracy in this case, it is possible to test that the simulation behaves properly with respect to the other variables governing the system. Examination of the effect of venting on the maximum pressure values is essential, when considering safety analysis.

The preliminary LSVCTF scenario was used to test the behavior of the code [11]. This included the 10m x 4m x 3m volume, a flame speed of 0.4 m/s in a central ignition

configuration. The vent sizes include: $0.56m^2$, $0.84m^2$, $1.12m^2$, and $1.4m^2$. Figure 4.10 represents the peak pressures produced at these varying vent sizes.

For comparison purposes, data collected by Molkov et al [16] was used. Their data is represented by Figure 4.14. The test scenario used by Molkov et al [16] is different from that of the LSVCTF. Still, the principles of vented deflagration remain. In both Figures 4.13 and 4.14, a trend is established with an increasing rise in peak pressure as vent size is deceased. The trend exemplified by the simulation are in agreement with the suggested hyperbolic relationship suggested by Mulpuru et al [10] Figure 4.15.

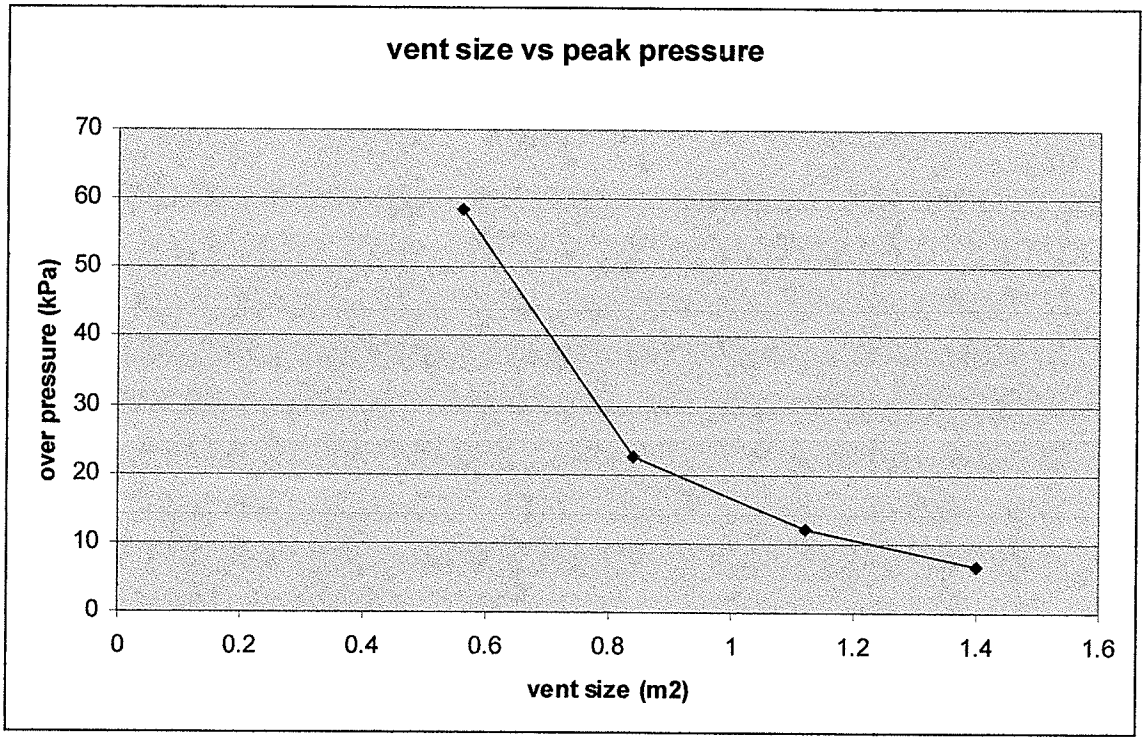

Figure 4.13. Vent Size vs Peak Pressure. Test 10m x 4m x 3m volume. Hydrogen concentration 11%, flame speed 0.4m/s.

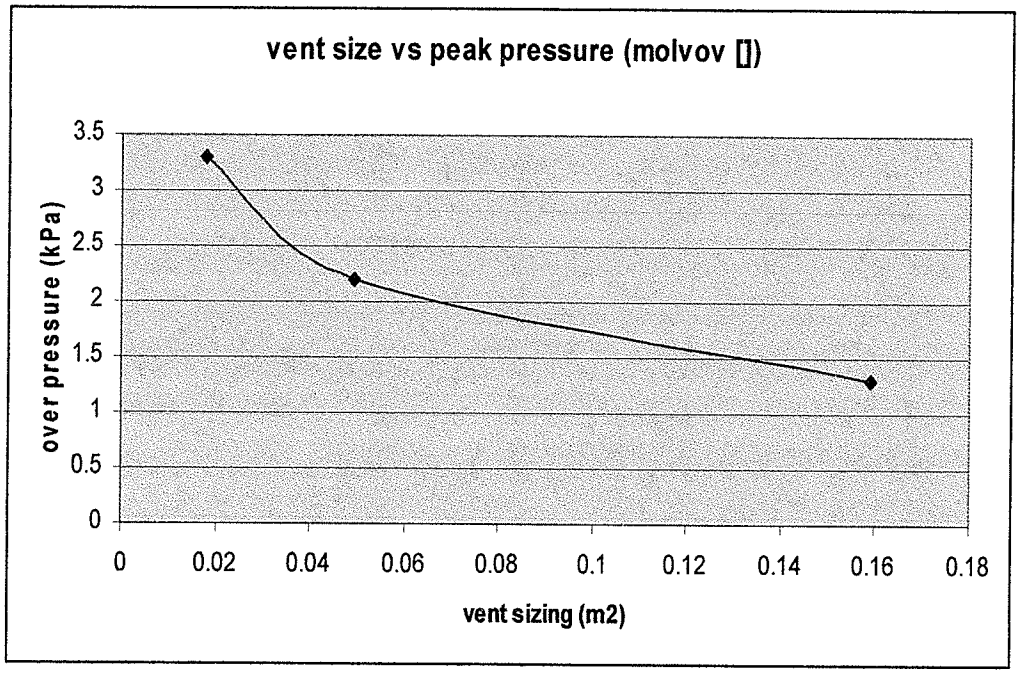

Figure 4.14. Vent Size vs Peak Pressure. Test 6.35m^3 volume. Hydrogen concentration 10%. Various vent sizes. Molvov [14]

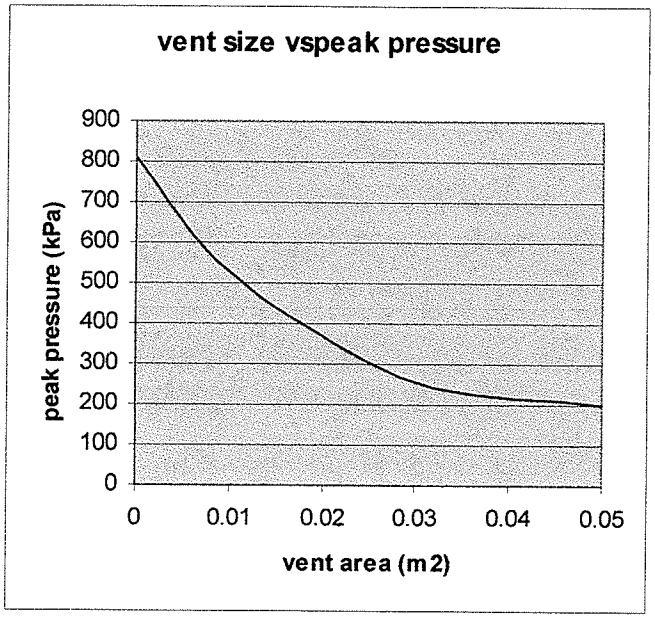

Figure 4.15. Vent Size vs Peak Pressure. Cylinder .775 m (h) x .504 m (d). Central Ignition. Hydrogen Concentration 40% Mulpuru [10]

LSVCTF Ignition Location Analysis

Ignition points were tested at varying distance from the vent. The collected data is presented in Figure 4.16. The peak pressure exists on the central ignition model, based on the mechanisms for pressure development. As demonstrated in Figure 4.4, central ignition provides the optimum use of space in all directions. This allows for maximum surface area and volume increase prior to the quenching of the flame front upon contact with the boundary walls. With ignitions closer to a boundary, quenching occurs sooner at one end of the flame, limiting the maximum surface area available (Figure 4.14).

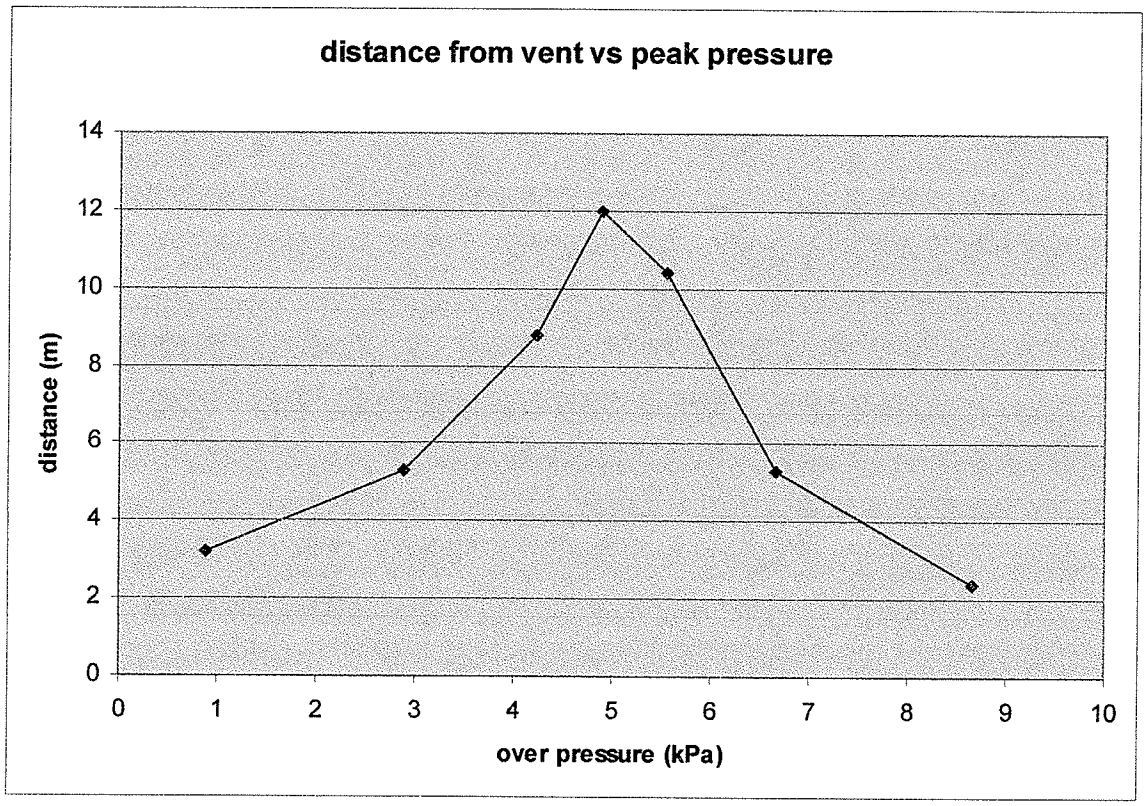

Figure 4.16. Ignition Distance from Vent vs Peak Pressure. Test 10m x 4m x 3m volume. Hydrogen concentration 11%, flame speed 0.4m/s.

Consider a closer look at the data from the tests with ignition points at 0.89m and 8.67m from the vent. Figure 4.17 provides the graphical representation of both flames. Figures 4.18 and 4.19 provide the respective pressure profiles.

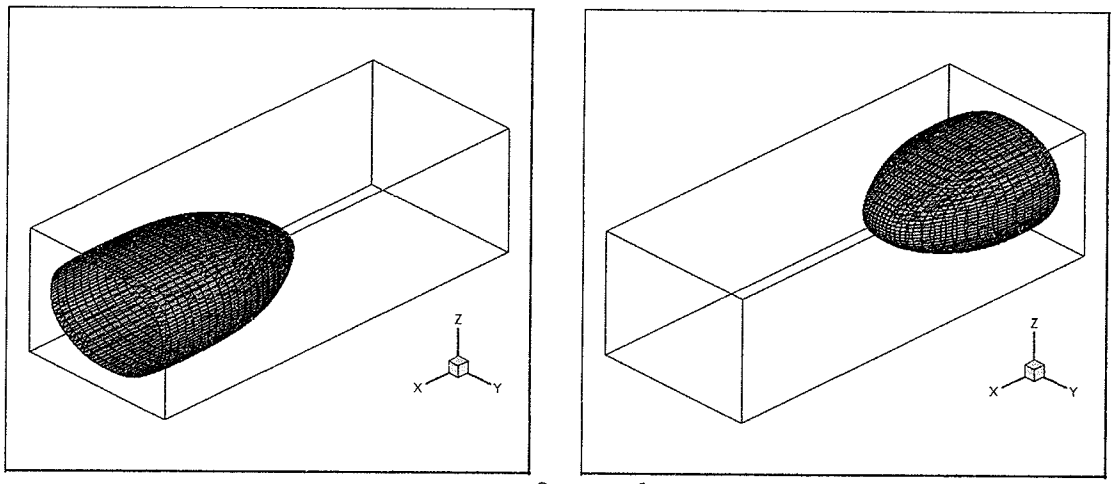

t= 8 seconds

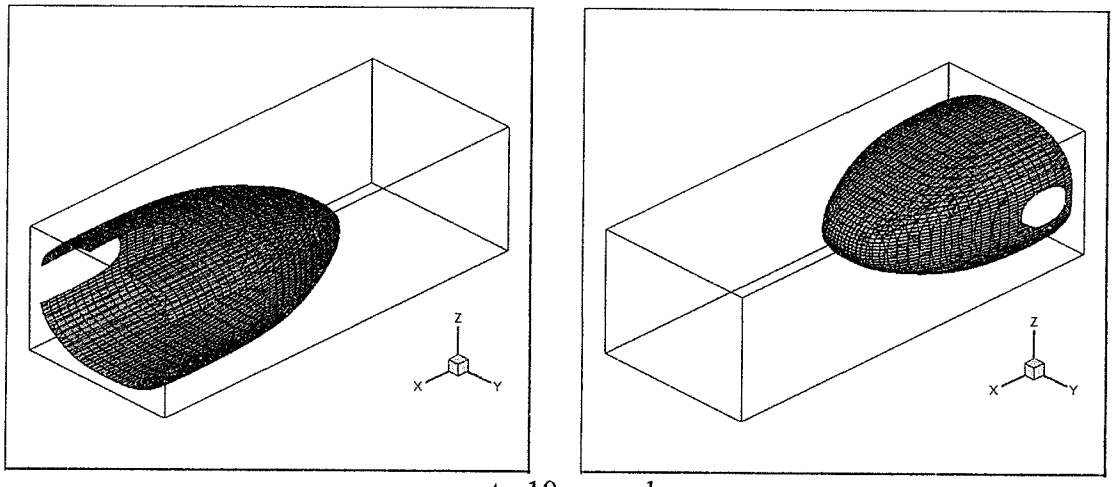

t= 10 seconds

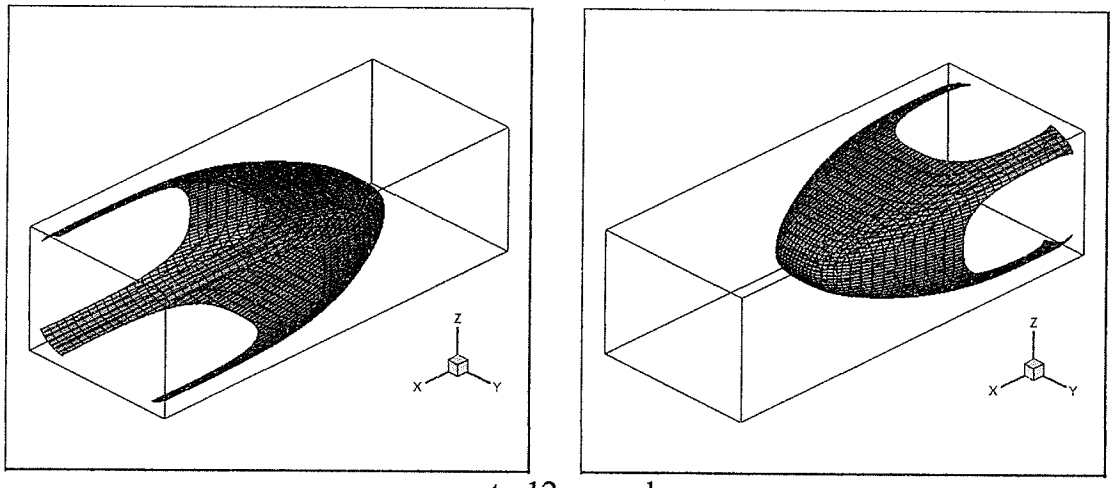

t= 12 seconds

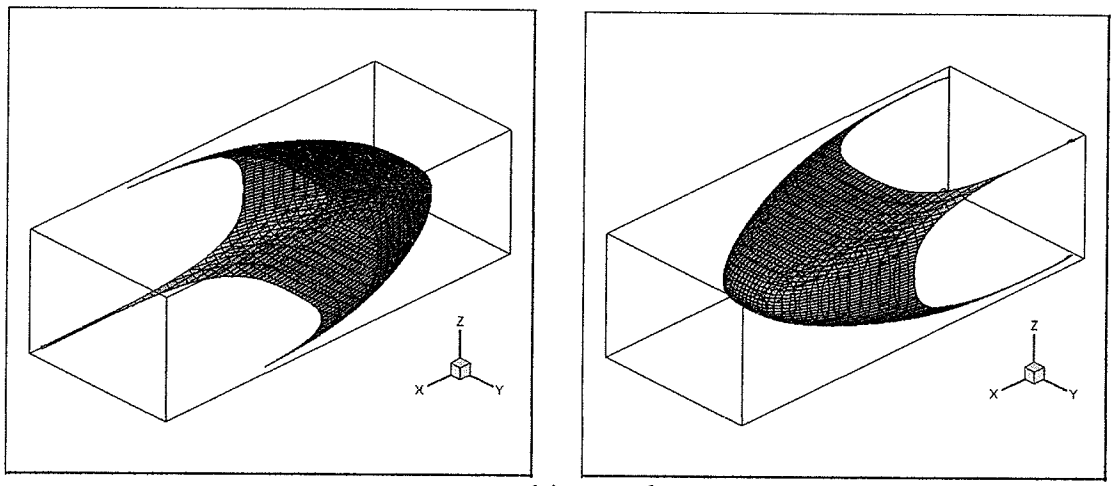

t= 14 seconds

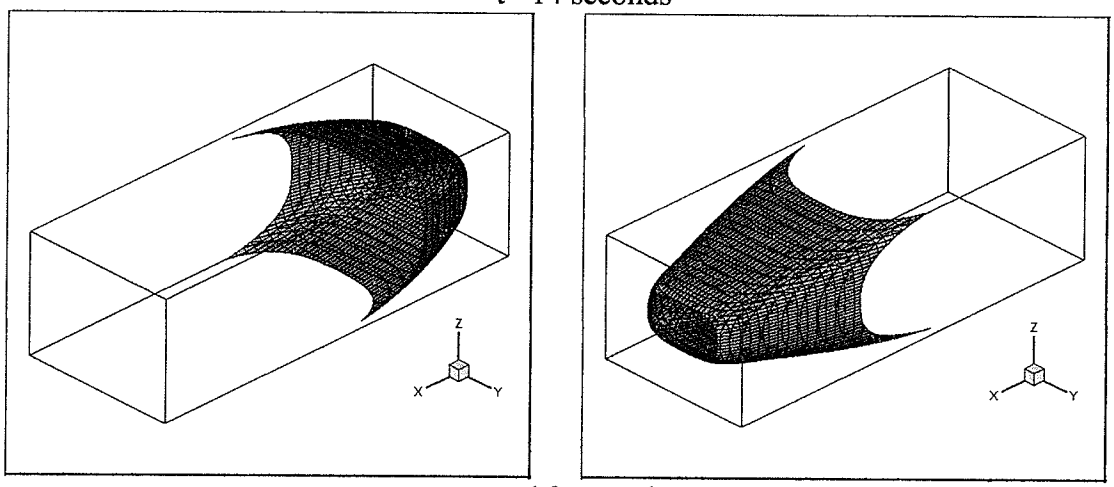

t= 16 seconds

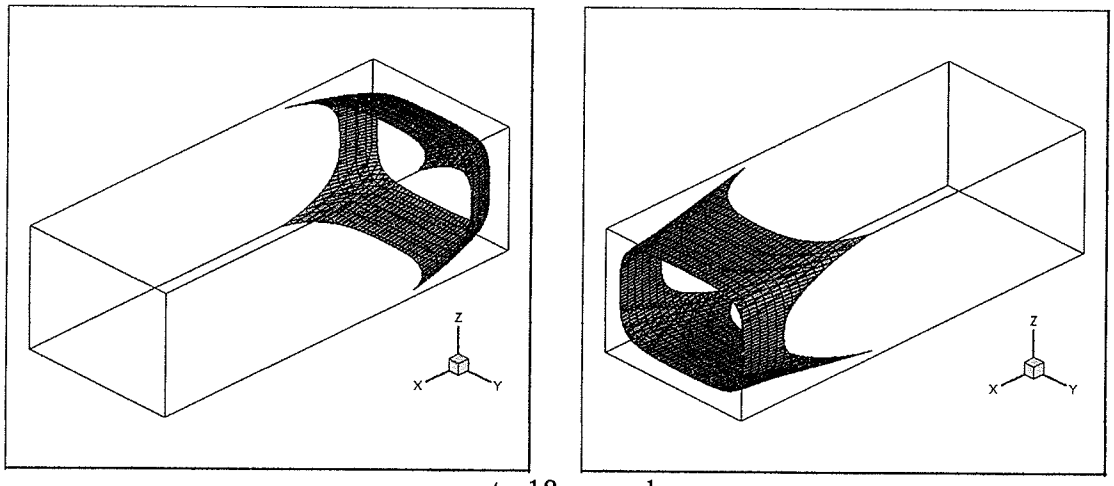

t= 18 seconds

Figure 4.17. Flame Representation. Test 10m x 4m x 3m volume. Vent size 1.05m x 1.05m. Hydrogen concentration 11%, flame speed 0.4m/s. near vent (left), near opposing wall (right)

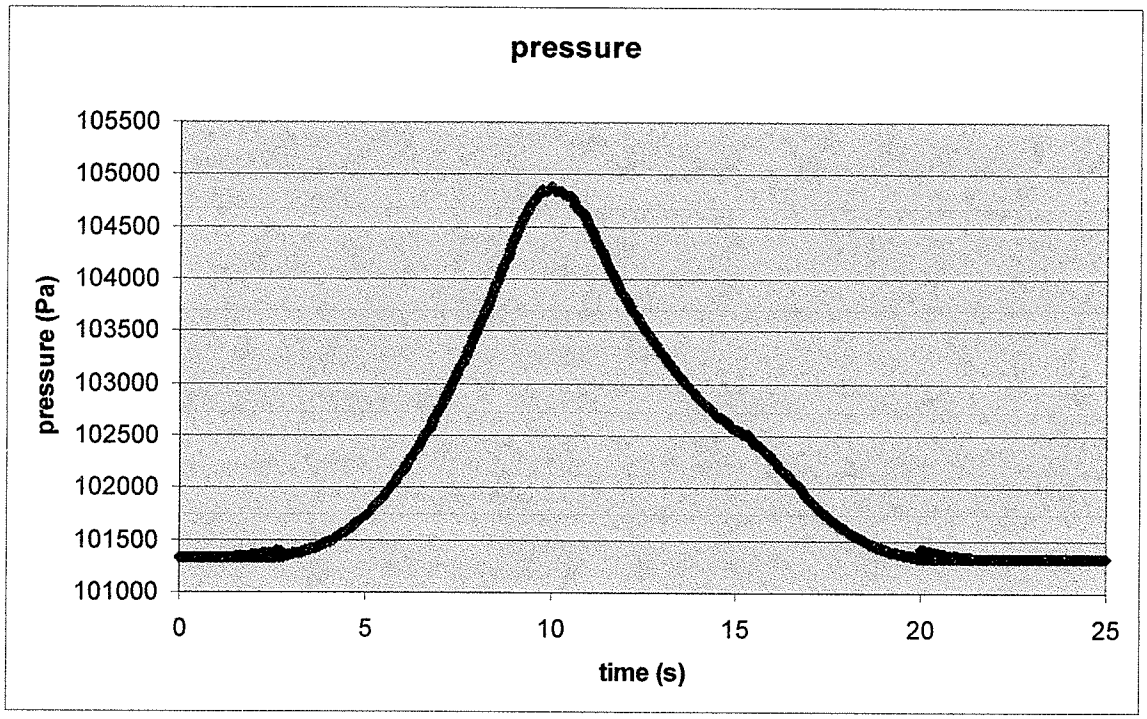

Figure 4.18. Pressure Profile. Test 10m x 4m x 3m volume. Vent size 1.05m x 1.05 m. Hydrogen concentration 11%, flame speed 0.4m/s. Near vent ignition.

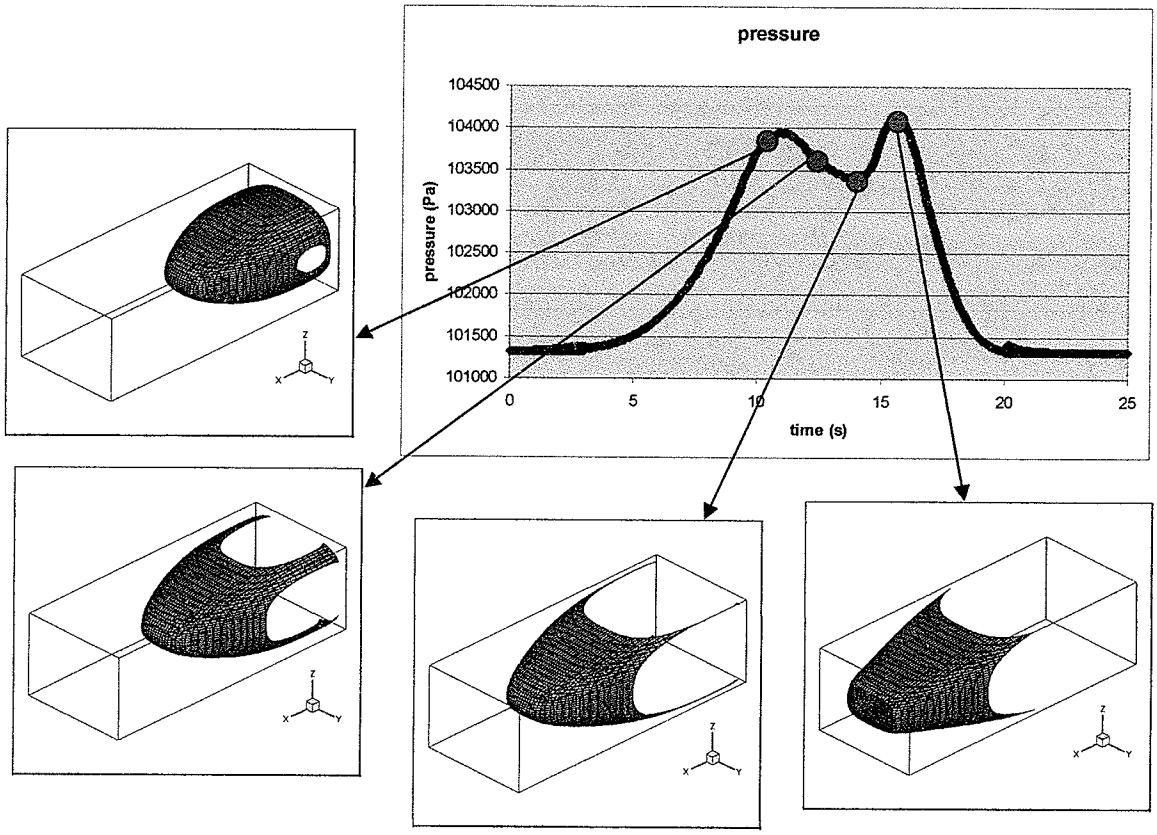

Figure 4.19. Pressure Profile. Test 10m x 4m x 3m volume. Vent size 1.05m x 1.05 m. Hydrogen concentration 11%, flame speed 0.4m/s. Near opposing vent ignition.

The results here continue to provide evidence concerning the lack of venting effects. Aside from the opposing ignition points, the two flames progress in a rather similar manner. It is not till 16 seconds (Figure 4.17) that clear indication of the vent effects appear. At this point there is a slight acceleration in the burning of the further ignition point test. Still, each test ends at approximately the same time. Sitar et al [11] discuss flame speed towards and away from the vent. Their data demonstrate that acceleration towards the vent is much more pronounced. The ability of this simulation to exhibit these effects is limited.

The effect of quenching is displayed in the pressure profiles of both tests. For both tests quenching by the nearby wall happens rather quickly. For the near vent combustion, the

peak is reached just as quenching begins against the surrounding volume boundaries (Figures 4.18 and 4.19). The opposing wall combustion behaves with multiple peaks (Figure 4.19). The initial peak occurs as quenching begins at the surrounding walls (Figure 4.17: t=10). The quenching continues and drive the pressure down as the flame surface is reduced (Figure 4.17: t=12). Eventual the quenching stops as a flame profile is defined along the profile of the volume (Figure 4.17: t=14). At this point there is no reduction is surface area as the flame travels down the remaining volume. During this time the pressure increases as fuel is consumed and flame cloud grows to increase the pressure within the volume. At this point the vent effects also begin to take shape, the stretching of the flame produces a further rise in pressure. Eventually, a second peak is formed demonstrating the ability of a vent to act as a mechanism for pressure generation. At the second peak (Figure 4.17: t=16), quenching at the vent wall begins effectively reducing flame surface area and pressure.

4.2.2. Cummings (HECTR and Conchas-Spray)

Experiments conducted for 15% hydrogen by Cummings et al [21] with HECTR estimated a total pressure of approximately 118 kPa over a 0.16 second interval. Conchas-Spray posted similar overpressures in a time of 0.16 seconds.

The replicated simulation is done with the simulation in this research, it converts the volume in Figure 4.2 with a cellular representation, depicted in Figure 4.20.

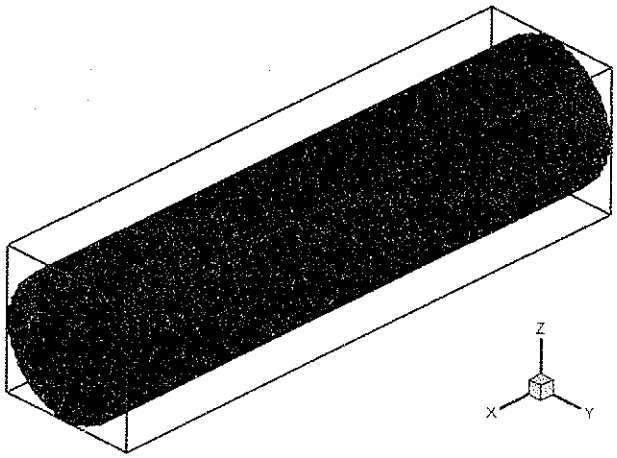

Figure 4.20: Representation of volume used by Cummings [21].

The initial simulation run conducted for 15% hydrogen proved unstable. A certain level of instability is expected at the beginning and end of the simulation where the changes in surface area and volume are small. These initial tests displayed instability throughout. Still, the recorded results of the simulation were 11.73 kPa, with a period of activity of 8.5 seconds. This is compared to the over pressure of approximately 17 kPa produced by Cummings [21]. The unstable pressure profile is presented in Figure 4.18. The issues with a lacking vent effect remain, signified by the lower pressure estimations and slower burn times.

Cummings [21] results for the same volume using 30% hydrogen produce approximately 175 kPa overpressures, with both HECTR and Conchas-Spray. Run times for both are approximately 0.08 seconds.The tests replicated by the simulation produced a peak over pressure of 105 kPa, running at approximately 2.4 seconds. Pressure and the surface area profiles for the test are in shown Figures 4.22 and 4.23. Flame representation is presented in Figure 4.24.

The long and narrow construction of the volume makes testing ideal for examining the effects toward the vent. There is a definite elongation towards the vent that is much more pronounced than in the results from the LSVCTF (Figure 4.7). The growth towards the

vent, though more apparent, is still insufficient. It is highlighted by the longer overall run time and the lower pressure levels.

As a cylinder with rounded walls, the flame reaches areas of the rounded boundary simultaneously. This leads to more dramatic quenching effects, signified by the steeper fall in surface area after achieving a peak at approximately 2 seconds.

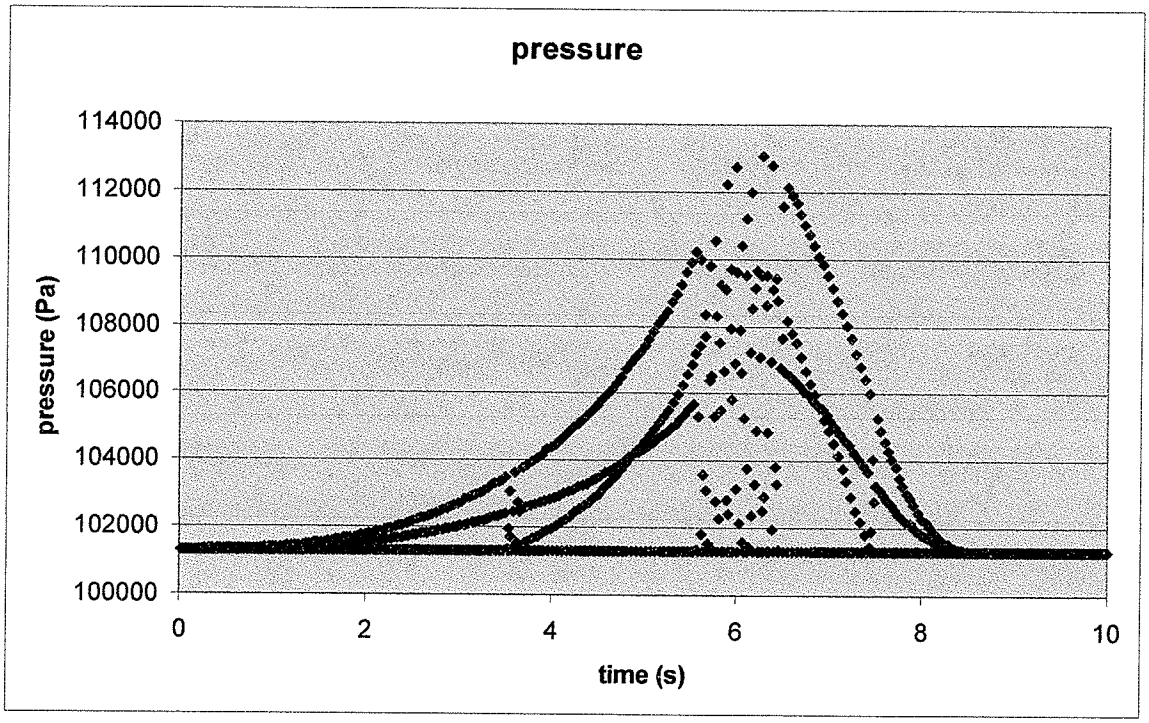

Figure 4.21. Pressure Profile. Test 4.88m (length) x 1.88 (diameter). Vent size .076m x 0.76 m. Hydrogen concentration 15%, flame speed 0.9m/s.

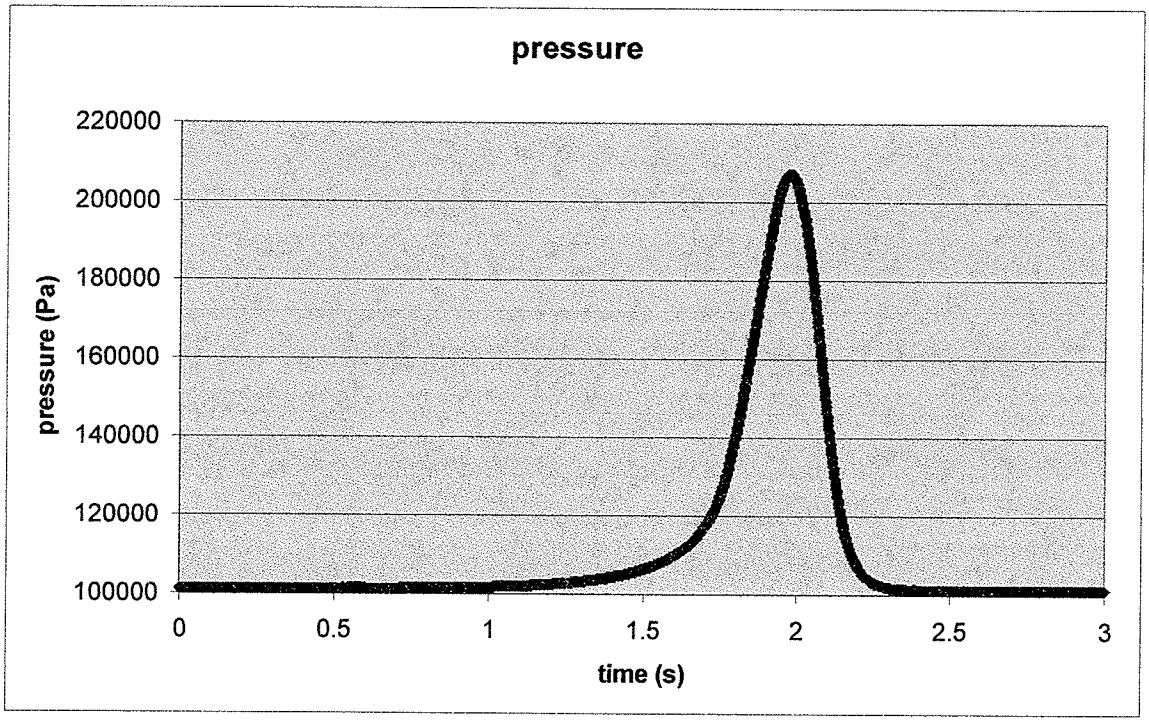

Figure 4.22. Pressure Profile. Test 4.88m (length) x 1.88 (diameter). Vent size .076m x 0.76 m. Hydrogen concentration 30%, flame speed 2.7m/s.

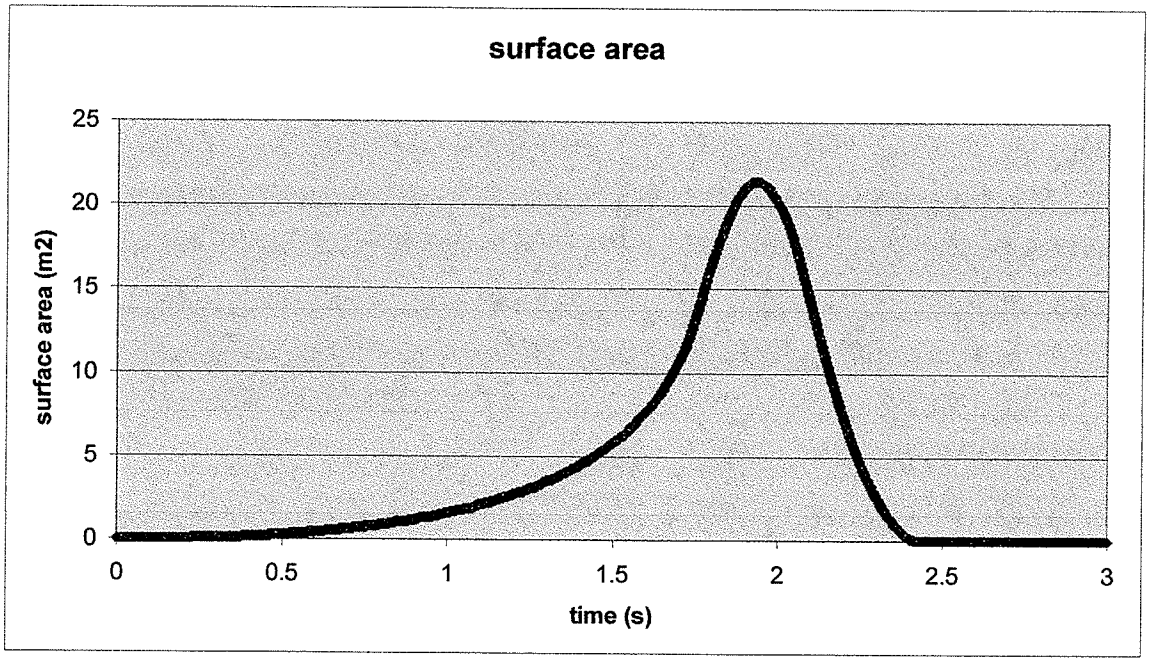

Figure 4.23. Surface Area. Test 4.88m (length) x 1.88 (diameter). Vent size .076m x 0.76m. Hydrogen concentration 30%, flame speed 2.7m/s.

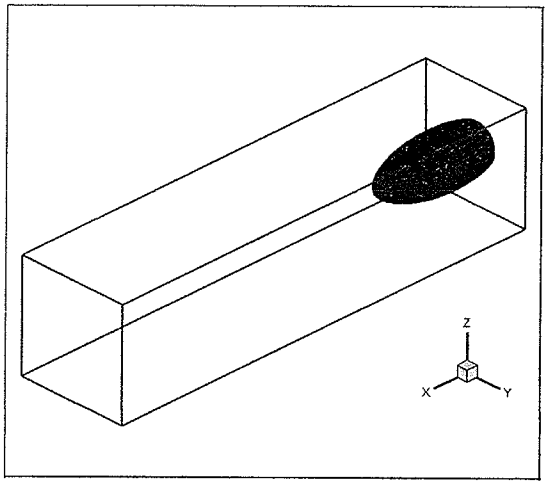

t= 1.0 seconds

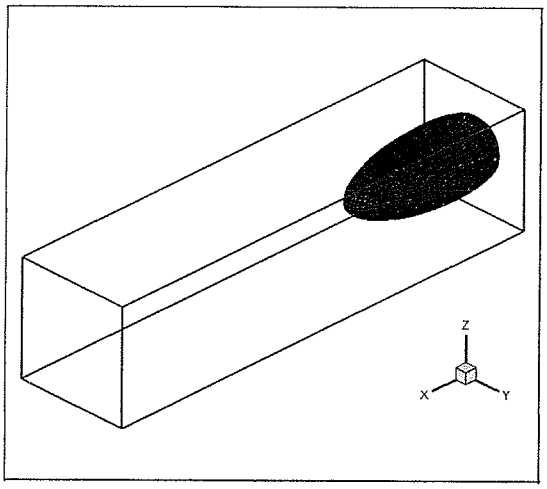

t= 1.2 seconds

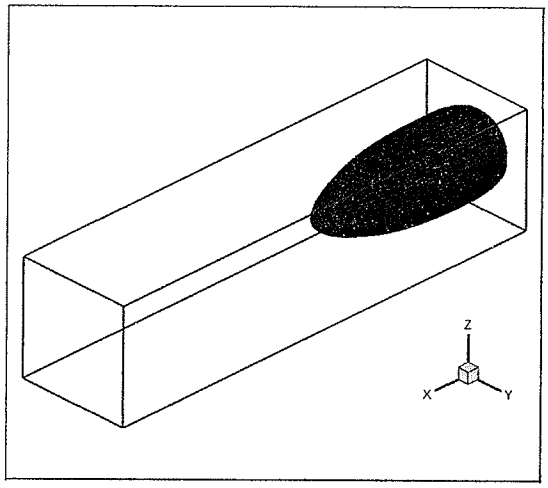

t= 1.4 seconds

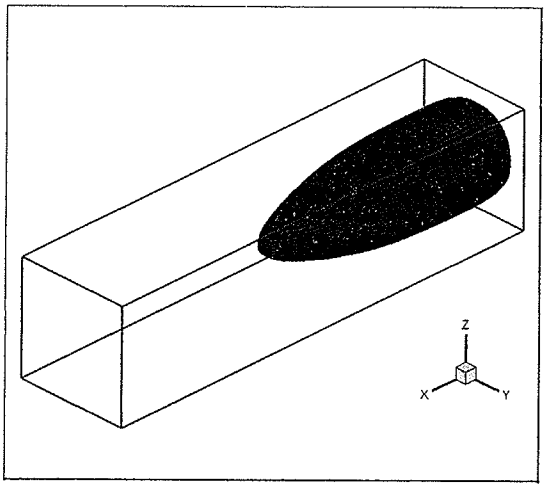

t= 1.6 seconds

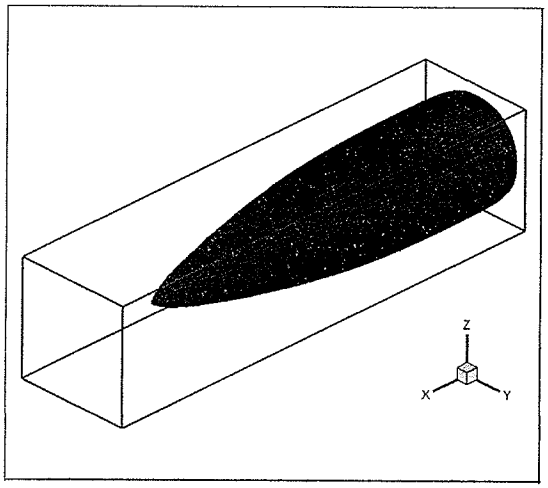

t= 1.8 seconds

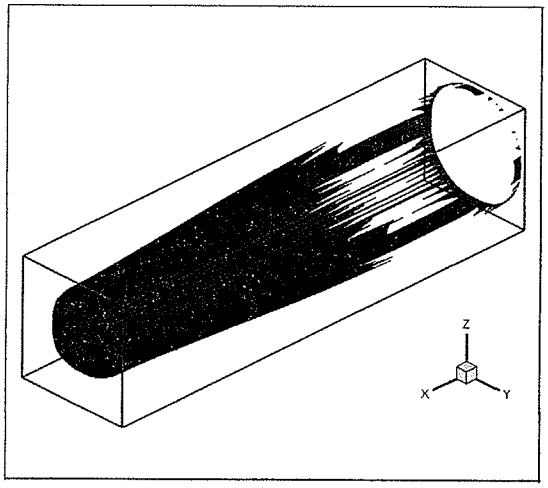

t= 2.0 seconds

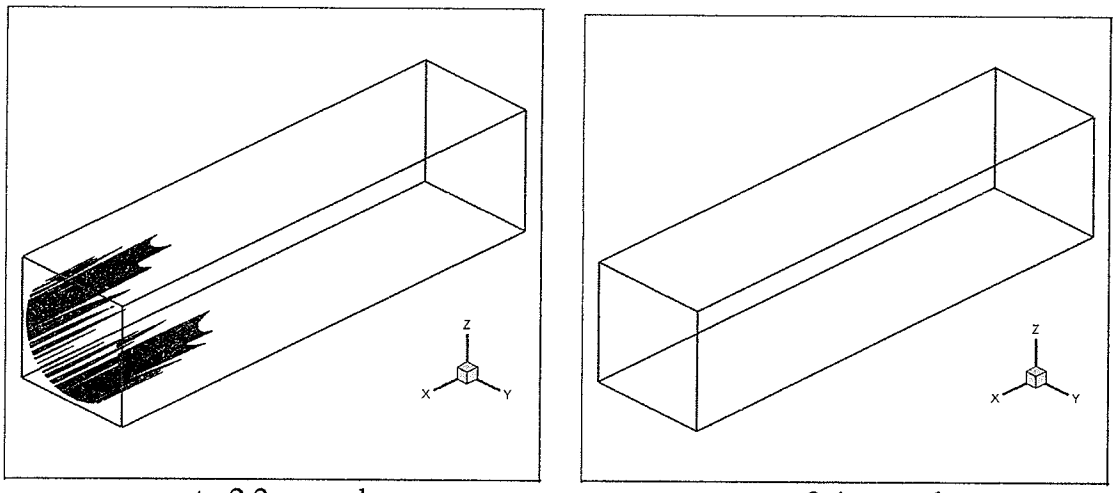

t= 2.2 seconds t= 2.4 seconds

Figure 4.24. Flame Representation. Test 4.88m (length) x 1.88 (diameter). Vent size .076m x 0.76 m. Hydrogen concentration 30%, flame speed 2.7m/s.

Chapter 5:

Web-based Simulation Implementation

5.1. VRML considerations

VRML (Virtual Reality Modelling Language) is language being capable of generating 3D geometry for web applications. Viewing of the simulation developed in this research is done through the use of a VRML viewer. A number of these viewers have become widely available for free across the worldwide web. Each viewer provides the user with the ability to navigate in the virtual space. This allows for thorough inspection of the generated geometry. Viewers can be used independently or can be imbedded in popular web browsers.

VRML itself provides limited interactivity within itself and other VRML files. Javascript can be incorporated into VRML to add increased functionality and interactivity. Programming languages can be interfaced with supported viewers, Java being the most readily available. Support for VRML is increasing across various programming platforms. As a display tool, the integration of VRML is steadily becoming ideal with its embedded user control, especially for applications stressing accessibility. Preliminary development of a VRML user interface for establishing and initiating the simulation is provided in Appendix B. Currently, the use of VRML has been to view visual output of the vented deflagration simulation.

The code generates VRML code for a few time steps in a simulation. A VRML script provides an interface for accessing each of the time steps one at a time, so that the progress of the simulation can be observed (Figure 5.1). The interface file allows for individual time step graphic files (Figure 5.2). Thus reducing the initial loading size, where each time step file can be requested individually, subsequently reducing a large file into a number of manageable segments.

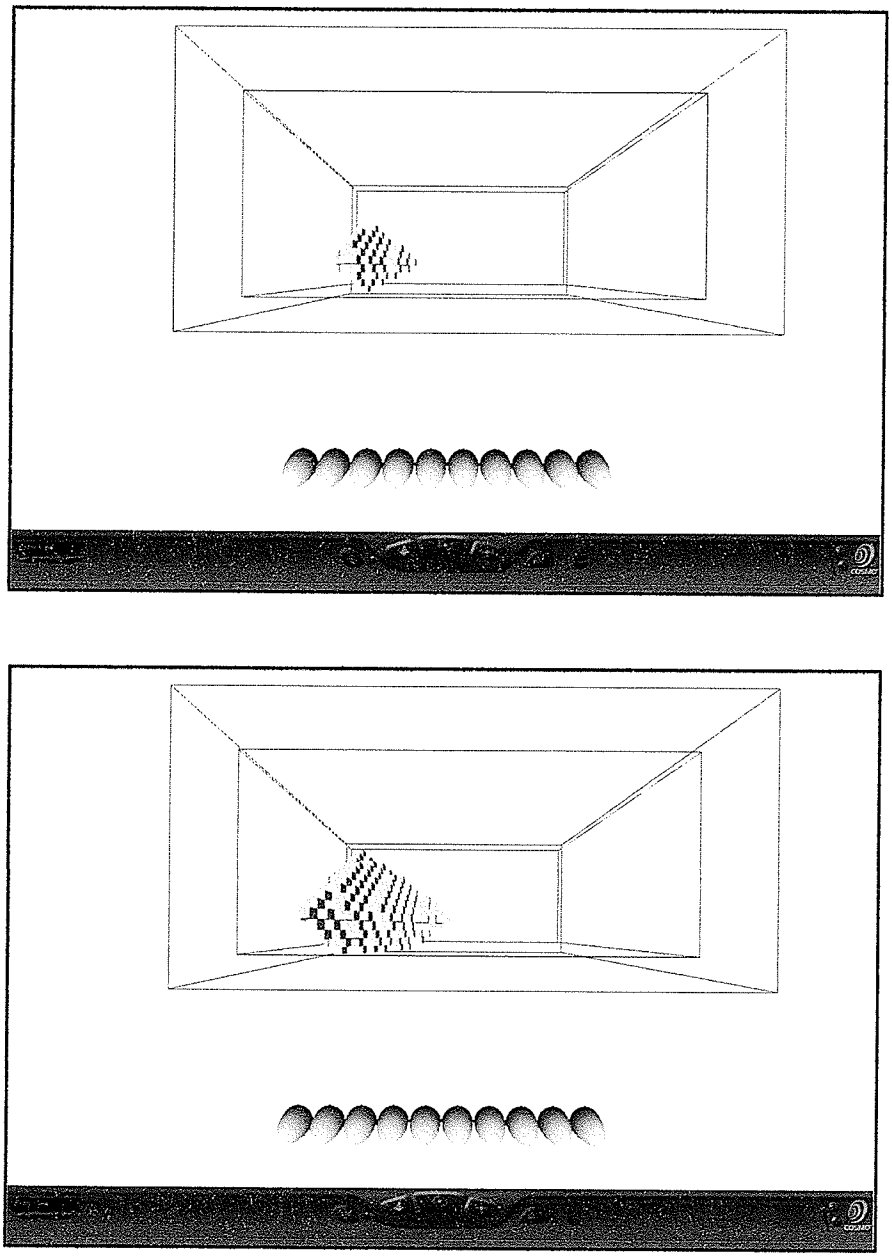

Figure 5.1: Simulation viewed in VRML

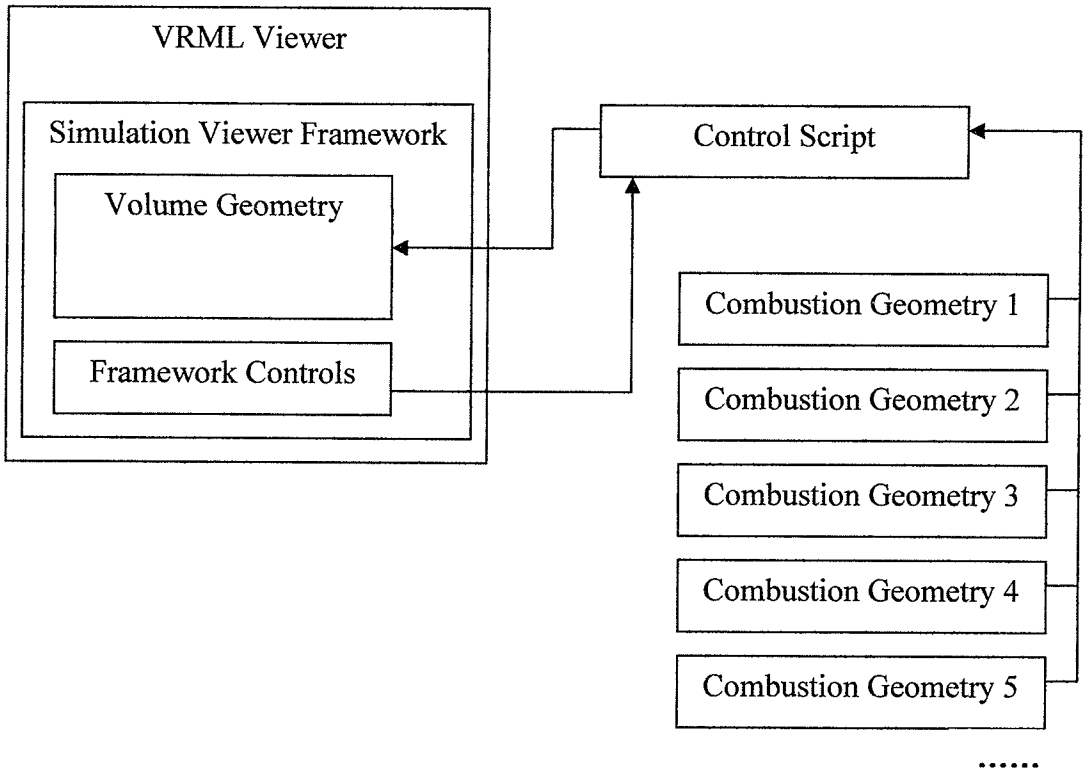

Figure 5.2: Simulation VRML Structure

Recently, VRML has been superseded by XML (Extensible Markup Language). XML provides support for previous VRML files. XML features increased support for scripting and programming to add functionality beyond viewing geometry. The support is unifying features that were once only available on specific VRML viewers.

5.2 Flash Considerations

Flash is an application that allows users to create animation for direct viewing or use on web pages. The use of flash is becoming a mainstay in overall web design. While the software's primary use is mainly aesthetic, users are quickly embracing the advantages of using Flash.

Flash allows developers to add increased interactivity to web interfaces, while providing an extra layer of security. Unlike, HTML and JavaScript, hyperlinks and source scripting are not transparent. Actionscript is an object oriented scripting language used in flash animations. Through Actionscripting, developers are able to provide advanced controls over the animations and pass information from other sources. This includes other programming languages and scripts, such as JavaScript.

The use of Flash for the deflagration simulation is to provide animations of the combustion process. Tecplot, the 3D plotting tool used here, has adopted the Flash animation. Prior animated output from Tecplot was either through the use of the windows media format, or raster meta files, which required a supplied viewer.

The raster meta files were able to maintain smaller file sizes and provides users control over the viewing of frames. Still, its use requires a proprietary viewer, not accessible web use. The window media format, is a file format that is web ready, and easily accessed through the use of the internet and common web browsers. It shortcomings come from its rather large file sizes and limited user control.

The addition of Flash support provides users with animation file format that is highly accessible through the Internet at relatively small file sizes. A flash animation is a series of images that act as frames. The animation can be established as a time sequence, or can collect a revolving camera view around a single time step. Animations for this simulation capitalize on both. The current output generated by Tecplot provides no user control, controls can be added using the Macromedia Flash Development. An ad hoc code can be used to extract frames from each times step and each available angle. The frames are inputted into a frame work in the Flash development software, that includes a user interface. The completed output presents the simulation data with controls for time and viewing angle (Figures 5.3 and 5.4).

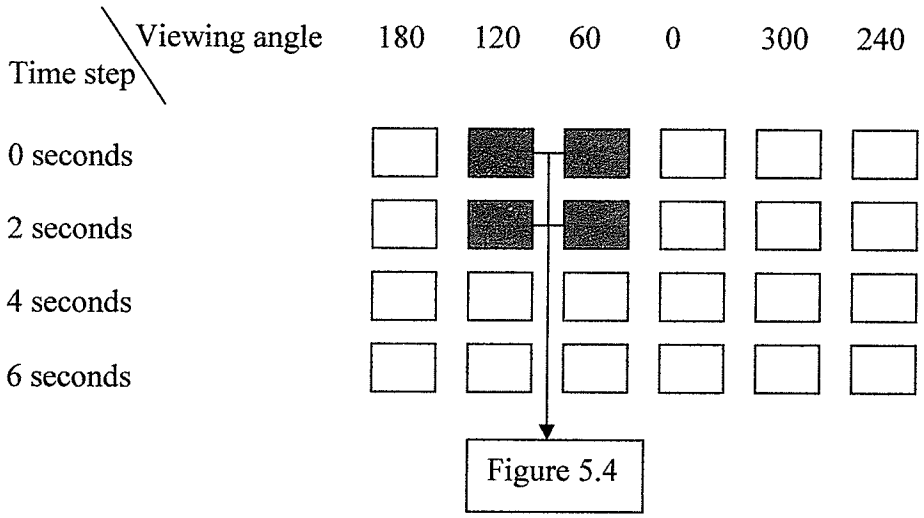

Figure 5.3: Flash Viewing Structure

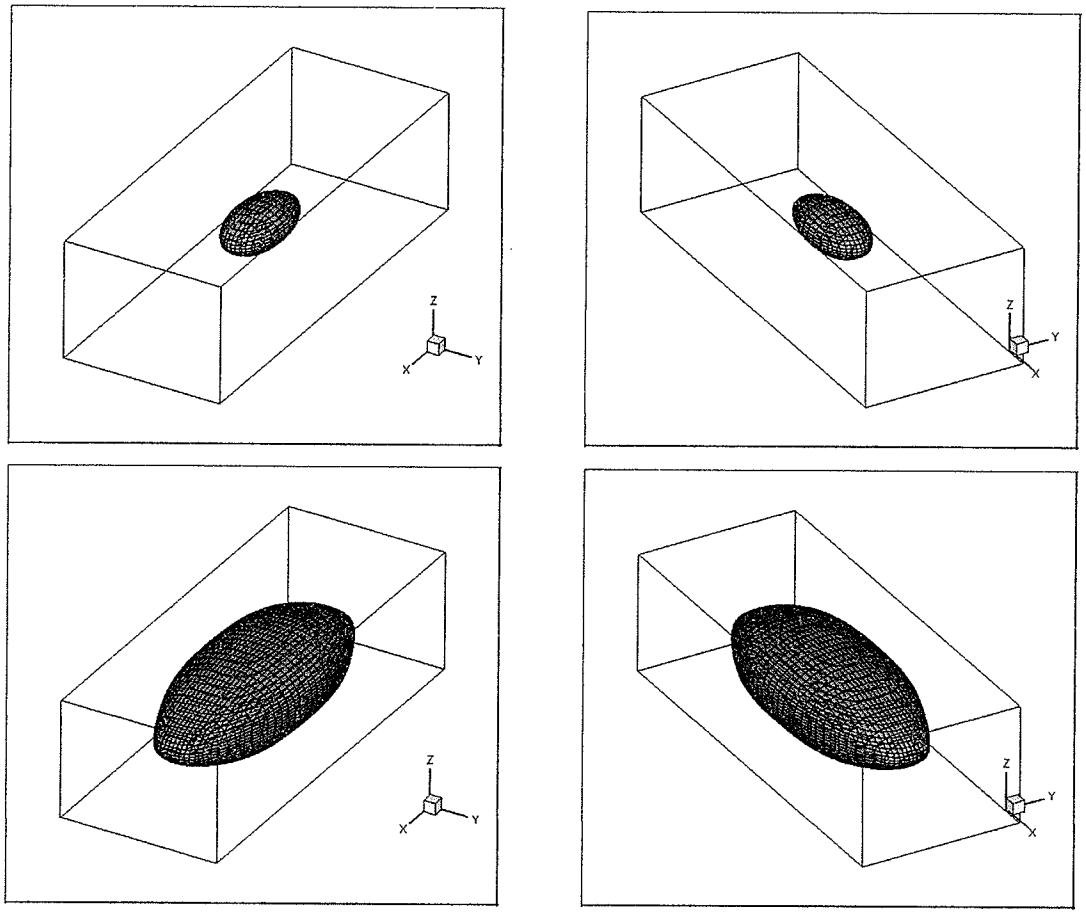

Figure 5.4: Flash Viewing Images

Chapter 6:
Conclusion and Further Work

6.1. Conclusions

The first notable area of progress was the straying away from the simple geometric analysis to allow for free form shapes. The finite volume and multiple burn directions let each portion of the flame react to the volume in a unique manner. The application of the flame tracking method has been successful, though the effect of the vent could be increased. The effects of diffusion, thermal expansion and vent effect can be clearly recognized.

The application and effective use of a finite volume approach has made it possible to apply 3D plotting techniques, specifically those provided by Tecplot. The flame can be observed as it propagates, both volume and surface area can be examined. The addition of graphics makes it possible to examine the relationships between the flame geometry, quenching and their effects on pressure development over the course of a deflagration.

Tecplot was further utilized for flash animation generation produce web ready visual output. VRML also provided web ready visual output. While still lacking a graphic interface, distribution through the web had not previously been explored. Initial development of a web based interface are provided in Appendix B.

The simulation does exhibit the proper behavior with respect to the mechanisms that produce pressure during vented deflagration. This includes increases in pressure as flame speed increased through changes in hydrogen concentration. The effect of vent size is represented through the reduction in pressure as vent size is increased. Changes in pressure caused by the movement of ignition locations follow the relationships suggested by Kumar [9]. Further insight can be gained by observing the flame behavior and

quenching patterns as ignition points are varied. This suggests the validity of the pressure estimation methodology and its application. Pressure values are generally lower than expected values, the suspected cause is the lacking vent effects. Increasing the vent effects would increase the rate at which flame surface is produced, thus increasing pressure rise and reducing active burn time.

As a generalized model, it was fully understood that this simulation could not compete with the level of depth and complexity provided by CFD. A generalized model, while lacking accuracy, gains the advantages of speed. Numerous tests could be completed in a relatively short time frame being able to quickly identify areas of concern. The simulation was initially intended to complement more complex numerical analysis, by reducing the range of necessary testing. Otherwise, the simulation could prove a valuable educational tool, highlighting the mechanisms of pressure development for vented deflagration.

6.2. Further Work

Vent effects

Based on the results of the testing conducted, there are clear shortcomings in the simulation, particularly in the modeling of the vent effects. This has been demonstrated both visually and by the recorded peak pressure values. These short comings can be attributed that concerns with the flame tracking methodology.

The fundamental equation for flame tracking (Equation 2.8) suggests three distinct components: the laminar burning rate, growth through thermal expansion, and growth through vent effects. Testing was conducted with the vent effect growth considered as the thermal expansion with no boundary. This would prove to be insufficient. Therefore a separate method for assigning vent effects would be required.

The deflagration code VENT, developed by Mulpuru et al [9], managed to apply vent effects as a ratio comparing the vent affected burn rate over the known laminar burn rate. This effectively acted as a multiplier to the burning rate. Within the VENT code this

concept was applied to an assumed spherical shape, in all direction equally. Applying the same methodology to the current simulation could nullify the unique flame shape generation. Application would have to be done with the consideration of burning directions.

Consideration of the test results from the Siter at al [11] from the LSVCTF implies that the effect of the vent on flame speed increases with proximity to the vent. The VENT code assumes a uniform growth.

To apply both principles properly, it is suggested that the application of vent induced flow be done with respect to a vector field towards the vent. Figure 6.1 displays a vector field based on the distance from the vent. Application of the vent induced flow would consider such a field with increasing effect as the vector becomes smaller.

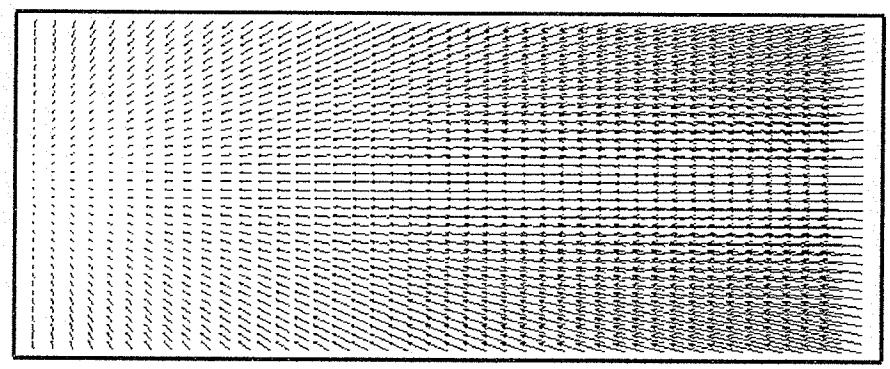

Figure 6.1: Vector field. Distance from the vent.

The use of the vector approach is also put into question when contrasted to the intercellular propagation of the current simulation. The current method only considers growth along the x, y or z directions. With a vent established along the x direction to the ignition point this would define vent flows equally along the entire yz plane. This would be unfavorable. A possible solution to this issue could be the comparison of another vector field based on the point of ignition. Another possible method involves using the vector angle as a possible gauge for scaling the effect of the vent induced flow.

A reasonable method for comparing the direction of the burn with the direction of the vent effects must be applied. Once established, other methods for estimating the value of vent induced flow can be employed.

Obstacles

The use of obstacles was a component of the original design of the simulation code. It was eventually dropped to focus on the proper application of the pressure development estimation. Multiple methods for applying obstacle effects were explored during the course of the research.

One method involves treating the free space left by an obstacle as a vent creating its on field of vent induced flow (Figure 6.2). The overall effect of the obstacle created vent is determined by its size and its relation to the true vent of the system. This would consider both proximity and position.

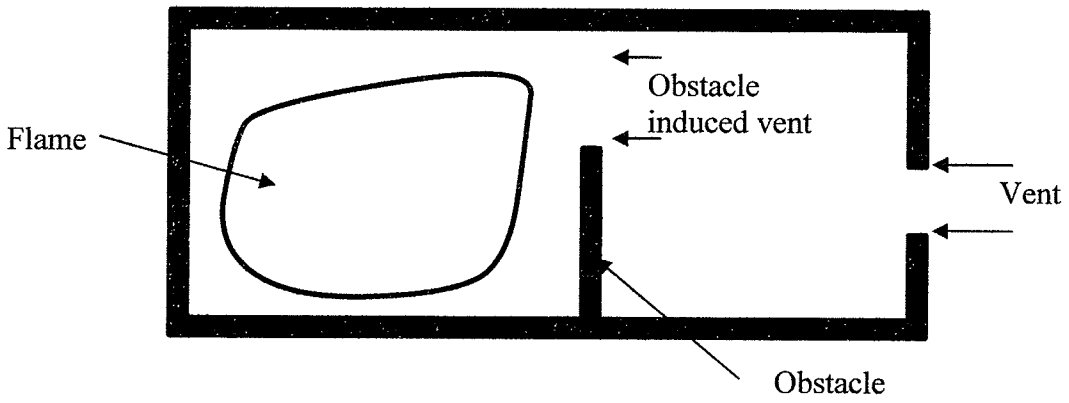

Figure 6.2: Obstacle Induced Vent

Another methodology considers the compressive effects on the thermal expansion of the flame. Growth of the burnt gas mass through thermal expansion is hindered both by the volume boundary and by obstacles. Values for this compression could be stored and reapplied as further expansion in areas not limited by boundaries or obstacles (Figure 6.3). One or both of these options could be considered when adding obstacles to the current simulation.

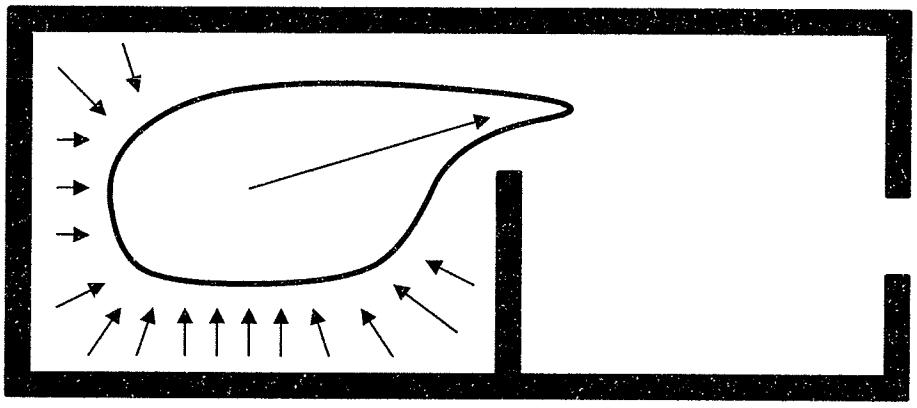

Figure 6.3: Compression to Expansion

Interface and Graphical Development

Initial development with VRML involved extensive use of the VRML for both interface and output generation, with the code existing as a client side backend to a VRML front. This initial development is highlighted by the work in Appendix B. Subsequently, the need to redefine the code removed this aspect of the research. Visualization in VRML would remain, as well as the addition of Flash output generation through Tecplot.

The addition of a graphical interface is still required to achieve complete web accessibility. Currently, the limited options do not require a high level of complexity to any proposed interface. As further options are added, especially the inclusion of obstacles, increasing level of 3D interaction will be necessary.

As an output option, the VRML portion is rather limited, where the data appears as a series of blocks. Sensitivity could be added to reflect the flame progress within each cell. Further development could yield iso-surface models similar to those produced through Tecplot, which would provide a step towards real-time generation.

References

[1] Breitung, W., Chan, C. K., Dorofeev, S. B., Eder, A., Gelfand, B. E., Heitsch, M., Klein, R., Malliakos, A., Shepherd, J. E., Studer, E. and Thibault, P. "Flame Acceleration and Deflagration to Detonation Transition in Nuclear Safety: State-of-the-Art Report by a Group of Experts" *OECD Nuclear Energy Agency. NEA/CSNI/R.* (2000)

[2] Parczewski, K.I. and Benaroya, V. "Generation of Hydrogen and Oxygen by Radiolytic Decomposition of water in some BWRs." *Designing for Hydrogen in Nuclear Power Plants.* (1984): 39-43

[3] Kumar, R.K. and Koroll, G.W. "Combustion Mitigation in Hydrogen/Air Mixtures by Dilution and Depletion Source." *American Society of Mechanical Engineers, Petroleum Division, 41, Emerging Energy Technology.* (1992): 45-52

[4] Chan, C. K. "Assessing the Possibility of Deflagration to Detonation Transition in a Non-uniform Mixture." *Proceedings of the 2003 International Autumn Seminar on Propellants, Explosives and Pyrotechnics - Theory and Practice of Energetic Materials.* (2003): 393-403

[5] Chan, C.K. and Dewitt, W.A. "Deflagration-to-Detonation Transition in End Gases." *Twenty-Sixth Symposium (International) on Combustion/ The Combustion Institute.* (1996): 2679-2684

[6] Lam, K.K., Wong, R.C. and Fluke, R.J. "Modelling of hydrogen mixing in a set of complex and connecting rooms in CANDU containment using GOTHIC." *Proceedings of the International Topical Meeting on Advanced Reactors Safety.* (1997): 589-601

[7] Tennankore, K.N., Koroll, G.W., Kumar, R.K., Lam, A.H.T., Chan, C.K., and Wren, D.J. "Hydrogen Combustion Issues and Containment Integrity." *Nuclear Containment. Proceedings of an International Conference.* (1988): 167-185

[8] Simpson, L.A. "Severe accident research in Canada." *Transactions of the American Nuclear Society.* (1994): 595-602

[9] Kumar. R.K., Dewit, W.A. and Greig, D.R. "Vented Explosion of Hydrogen-Air Mixtures in a Large Volume." *Proceedings of the 1987 ASME-JSME Thermal Engineering Joint Conference.* (1987): 297-304

[10] Mulpuru, S. R. and Wilkin, G. B. "Model for Vented Deflagration of Hydrogen in a Volume." *At Energy Can Ltd Rep. Canada.* (1982)

[11] Loesel-Sitar, J., Koroll, G.W., Dewitt, W.A. and Bowles, E.M. "The Large Scale Vented Combustion Test Facility at AECL-WL: Description and Preliminary Results." AECL-11762. *AECL Whiteshell Laboratories, Pinawa.* (1997)

[12] Sato, Y., Iwabuchi, H., Groethe, M., Merilo, E. and Chiba, S. "Experiments on Hydrogen Deflagration." *Journal of Power Sources.* (2006): 144-148

[13] Molkov, V., Dobashi, R., Suzuki, M. and Hirano, T. "Venting of Deflagrations: Hydrocarbon-air and Hydrogen-Air Systems." *Journal of Loss Prevention in the Process Industry.* (2000): 397-409

[14] Molkov, V., Dobashi, R., Suzuki, M. and Hirano, T. "Modeling of Vented Hydrogen-Air Deflagrations and Correlations for Vent Sizing." *Journal of Loss Prevention in the Process Industries, 12.* (1999): 147-156

[15] Bradley, D. and Mitcheson, A. "Venting of Gaseous Explosions in Spherical Vessels EM Dash 1. Theory and Experiment." *Combustion and Flame.* (1978): 221-236

[16] Bradley, D. and Mitcheson, A. "Venting of Gaseous Explosions in Spherical Vessels EM Dash 2. Theory." *Combustion and Flame.* (1978): 237-255

[17] Swift, I. "Gaseous Combustion Venting - A Simplified Approach." *Institution of Chemical Engineers Symposium Series.* (1983): 21-37

[18] Swift, I. "Vented Deflagrations – Theory and Practice." *Plant/Operations Progress.* (1984): 89-93

[19] Fairweather, M.and Vasey, M. W. "Mathematical Model for the Prediction of Overpressure Generated in Totally Confined and Vented Explosions." *Symposium (International) on Combustion.* (1982): 645-653

[20] Whitehouse, D.R., Loesel-Sitar, J. and Chan, C.K. "A Novel Approach to Vented Combustion." *Atomic Energy of Canada Limited. Containment Analysis Branch.* (1996)

[21] Cummings, J. C., Lee, J. H. S., Marx, K. D. and Camp, A. L. "Analysis of Combustion in Closed or Vented Rooms and Vessels" *Plant/Operations Progress, volume 3.* (1984): 239-247

[22] Lee, J., Lee, Jin-Yong; Park, G., Lee, B., Yoo, H.; Kim, H. and Oh, S. "Gothic-3D Applicability to Hydrogen Combustion Analysis." *Nuclear Engineering and Technology, 37.* (2004)

[23] Baraldi, D., Heitsch, M. and Wilkening, H. "CFD Simulation of Hydrogen Combustion in Simplified EPR containment with CFX and REACFLOW." *Nuclear Engineering and Design.* (2007): 1668-1678

[24] Manninen, M., Silde, A., Lindholm, I., Huhtanen, R. and Sjovall, H. "Simulation of hydrogen Deflagration and Detonation in BWR Reactor Building." *Nuclear Engineering and Design.* (2002): 27-50

[25] Kirby, D.C. and Schwab, R.F. "Report of the Committee on Explosion Protective Systems." (2001)

[26] Kirby, D.C. and Schwab, R.F. "NFPA 68 Guide for Venting of Deflagrations 2002 Edition." (2002)

[27] Koroll, G.W., Kumar, R.K. and Bowles, E.M.. "Burning Velocities of Hydrogen-Air Mixtures." *Combustion and Flame*, 94. (1993): 330-340

Appendix A:

Graphical Work at AECL

A.1. Introduction

GOTHIC, DDTINDEX and Tecplot have previously been employed to perform DDT analysis on possible accident scenarios with success (Figure 1). GOTHIC and DDTINDEX are applications that derive information pertaining to the simulation of a LOCA. To perform graphical analysis, Tecplot was used. Under consideration is an effective way of examining and demonstrating results graphically, specifically in three-dimensions.

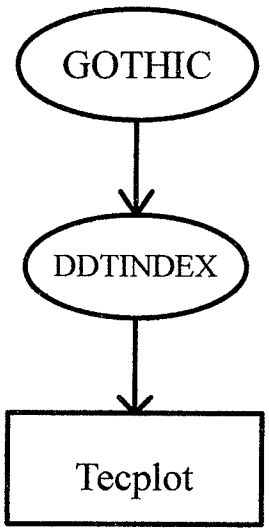

Figure 1: Using GOTHIC, DDTINDEX and Tecplot

A.2. GOTHIC

GOTHIC is a thermal hydraulic code designed to simulate multi-phase and multi-flow systems. Developed by NAI (Numerical Application Inc.), GOTHIC is capable of simulating continuous gas and liquid flows, along with drops, though various systems in

one-dimensional, two-dimensional, or three-dimensional environments. The basis of GOTHIC is under the fundamentals of the conservation of mass, energy and momentum. The code is used to simulate gas flows and record gaseous properties through a model of a volume.

Under previous work, GOTHIC was used to develop a model of a CANDU facility. A number of control volumes were created in GOTHIC to represent the various rooms within the facility. Control volumes can be constructed in two ways: lumped parameters and sub-divided volumes. In lumped parameter volumes data are available for the entire volume. Therefore, a hydrogen concentration value will represent the concentration of the entire volume. Sub-divided volumes are generated by a three-dimensional grid. Here simulated data represent each sub-volume defined by this grid. This method of defining a volume can reveal additional information concerning the distributions of values. In order to reproduce the associations found in thermal hydraulic systems, volumes can be joined to allow for flow between them. The numerous control volumes created to represent spaces in the facility can be connected so that the movement of the gaseous mixtures within the structure could be replicated.

By establishing the entrance of heated gases within the model a LOCA could be simulated. It is the behavior of these gases within the modeled environment that is of concern. GOTHIC can replicate the behavior of these gases tracking the concentrations and properties of hydrogen and steam throughout the CANDU model. Varying the locations of this sudden entrance of gases defines the type of LOCA scenario being modeled and the overall results of the simulation.

Analysis of gas distributions is vital in specified areas of the CANDU model for specific reasons, including the overall size of the areas, the role played by these volumes, and the expected concentrations of the volatile gas mixture in a LOCA situation. The added interest in these areas, warrants that the controlled volumes be defined as sub-divided volumes so that the concentration distributions can be studied with more depth. The two spaces can have a direct relation to the location of the rupture causing the LOCA, making

in depth examination of these areas valuable. Also, being of significant size, values for concentrations of gases cannot be properly represented as a lumped parameter volume. All other areas are represented by lumped parameter values.

Once a simulation is run in GOTHIC, data can be extracted as specified. The user can select which volume data is required for, which data (ie. temperature, gas concentrations, pressures, etc.) and time properties of the data. Time properties include the start and end time of the data, along with the time step at which data should be output. The data file produced is an ASCII data file containing values corresponding to the specified variables at the required times. For subdivided volumes the data file contains a set of tables, one for each time step, that contain the Cartesian co-ordinates for locations within the selected space and matching values for the specified properties. The formatting of the output data is such that it is compatible with Tecplot.

Values for hydrogen, steam and temperature concentrations during the simulation are the necessary data extracted from the simulation.

A.3. DDTINDEX

DDTINDEX is a supplementary code that is coupled with GOTHIC for the purposes of examining the potential a DDT within a simulated system. DDTINDEX is designed to accept output data from GOTHIC, specifically the ASCII data files tailored for use in Tecplot. DDTINDEX is able to accept both lumped parameter and subdivided volume data. Interest lies in subdivided volume information.

The purpose of DDTINDEX is to analyze the GOTHIC simulated data and return values for DDT Index, FA Index, DDT Potential, and FA Potential. These four parameters act as indices to the possibility of a DDT based on the current distribution within the volume.

A.3.1. DDT Index

As hydrogen enters the room, the heightened levels identify gas clouds within volume. Based on the concentration of hydrogen, steam and the size of the cloud it can be judged whether the atmospheric conditions are available for a DDT reaction.

The method at which DDTINDEX solves for this problem is by first compiling a cloud of hydrogen gas at each time step. This is accomplished by examining the hydrogen percentage at each point. Once compiled an overall cloud size can be calculated, more specifically a cloud length. At each point the value of hydrogen and steam concentration determine a detonation cell size, which acts a gauge for the reactivity of the gas mixture. This cell size is compared with the cloud length. If the cloud length is less than seven times of the detonation cell size the conditions for a DDT are satisfied. Therefore, the smaller the cell size, the greater the reactivity.

A.3.2. FA Index

Flame acceleration is a vital component of a DDT. The determination of FA Index is through the analysis of the expansion ratios between unburnt gas and burnt gas, defined by the density of both gases at the reaction front. In the deflagration regime this expansion ratio acts as an indicator of the burning rate. Levels of hydrogen concentration, steam concentration and temperature are related to value of this expansion ratio. By assuming all points in the volume are at the reaction front, an expansion ratio can be solved for all cells.

FA Index is a comparison of the solved expansion ratio compared to a critical value for the expansion ratio. If the solved value is greater than the critical value, the conditions of flame acceleration for a DDT are satisfied.

A.3.3 DDT Potential

A DDT is not instantaneous, it is a process that develops into a detonation. There is a distance associated with this process in terms of the location of ignition and the location of the onset of detonation. This distance is referred to as the run-up distance. For a detonation to occur from a deflagration state this minimum distance must be met.

DDT run-up distance is related to the concentrations of both steam and hydrogen in a gaseous mixture. Run-up distances are determined for all points in the data file and these values are indexed against the cloud length at that particular time. DDT Potential is the ratio produced by this comparison. If the cloud length is longer than the run-up distance then this criteria for DDT is fulfilled.

A.3.4 FA Potential

Flame acceleration run-up is the distance between a point of ignition and the point of onset of a supersonic flame. FA run-up distance values are related to the hydrogen and steam concentrations in a gaseous mixture. The ratio of FA run-up distance and the cloud length is FA Potential.

FA Potential is much like DDT Potential. Values for run-up distance are solved at all available data points in the volume and from these FA Potential can be solved. If the cloud length satisfies the FA run-up distance there is possibility for a DDT.

The four indices are all ratios of critical factors, each suggesting that a condition is satisfied. All must be satisfied for the possibility of a DDT. For all, having a value of one implies that the critical value is reached and any value greater would increase the probability for a detonation from deflagration.

DDTINDEX solves for the indices for each cell in a subdivided volume, as it is defined in GOTHIC. Output from DDTINDEX is formatted in the same structure as the data file from GOTHIC. The number of data points, however, has been reduced. Solved values for the indices are for each cell data is presented only for the cell centers.

A.4. Data Format

GOTHIC and DDTINDEX both create output data in the same format for subdivided volumes. This format is referred to as "IJK ordered data." The name describes the structure that the data is presented in.

A single data point is represented as a list of figure on a single line. The first three values are the x, y, z co-ordinates of the data point. Following the co-ordinates are the values of the data stored at this point. Values can be of any property (ie hydrogen concentration, temperature, etc.) and there can be any number of properties represented, the only requirement is that all data points be consistent. Therefore, the first three values for each data point must be the location, the next can be any one property, followed by another property and can continue indefinitely. Every data point must hold values for the same number of properties and all properties must be in the same place in all data points. Labels for the properties are provided through a header at the beginning of the data file, these are organized in the same order values are presented for a data point.

The GOTHIC model, in terms of subdivided volumes, is defined by a three-dimensional grid that creates an array of rectangular cells. The data file will contain a number of data points defined by this construction. It becomes important to understand the difference in data placement between GOTHIC and DDTINDEX output.

The model in DDTINDEX is represented as cell center data. The data file produced contains information only for the geometric centers of each cell. Therefore, there is only one data point for each cell (Figure 2a). A consequence of this method of representation is that the data do not extend to the geometric limits of the volume.

When producing output GOTHIC presents data for all cell centers, all face centers, all vertices, and all edge centers. The result of this is that each cell is represented by a total of 27 data points (Figure 2b). Of these points, 26 are shared with adjacent cells, the

remaining is the cell center. GOTHIC data files are capable of displaying the geometric limit of the volume.

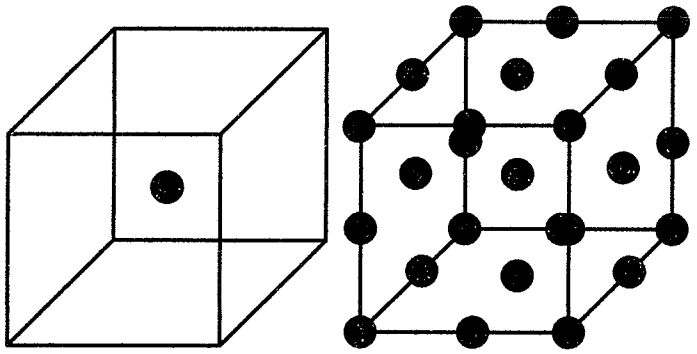

(a) (b)

Figure 2: (a) cell-center data, and (b) GOTHIC representation

Regardless of the application generating the data file, the arrangement of data points must remain consistent. As the name suggests the data points must be ordered by location. Points are organized by the x axis, then by the y axis and finally by the z axis.

A simulation takes place over a chosen time period. GOTHIC allows a user to specify a time range and a time step. At every time step within the time range, GOTHIC will output values of the properties required for the entire volume. Therefore, an entire representation of the volume will be generated repeatedly. Each completed time step is printed sequentially in the data file as zones. Examining changes between zones can describe patterns and movement of distributions over time. Every zone is labeled by number, and optional text. Other valuable information given in the zone label are the number of data points given in each axial direction and the format of the data stored. Data can be presented in other formats, but for the purposes of this study, IJK ordered data is the most suitable.

A.5. Tecplot

Tecplot is a multipurpose plotting program capable of graphically displaying data in different formats. Data files from GOTHIC and DDTINDEX are accepted formats in

Tecplot. With three-dimensional IJK ordered data, Tecplot is equipped with various features that aid in the illustration of data for the purposes of examination. Tecplot has proven to be a very able tool for developing graphics that properly represent the output.

A.5.1 Mesh and Boundary

The mesh feature illustrates the geometry of an IJK ordered data set by generating a grid with all the data points acting as vertices (Figure 3). Meshing helps identify locations in the volume as well as the placement of data and planes in the I, J, or K directions. A generated mesh will also, define the limits of the data. To highlight these limits further the boundary feature can be used.

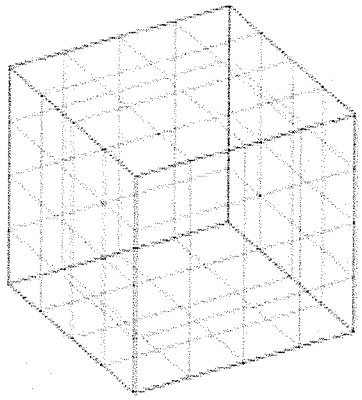

Figure 3: mesh

DDTINDEX output contains data at the cell center, therefore the cells formed by meshing of this output will not properly represent the volume under analysis properly. With GOTHIC output, because of the extended number of data points, a model cell will appear as eight adjacent cells when the mesh feature is used.

A.5.2. Contours

Contours are two-dimensional planes that coincide with the planes defined by the data file in its IJK ordering. Contour planes can account for the distribution of one property defined in the space. They present a topographical view of the data as slices of a three-

dimensional space (Figure 4). Typically, a spectrum of colors can be applied to data that has been segmented into successive ranges. A legend can be provided to explain the association of color and data values. If the use of colors is undesirable or insufficient, outlines can be used to further distinguish between regions of data.

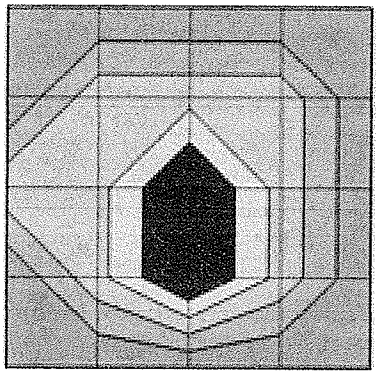

Figure 4: contour plane

A.5.3. Iso-surfaces

Contouring associates a color to data belonging to a range of values, iso-surfaces create a surface that surrounds data of a specified range. Figure 5 illustrates iso-sufaces produced from the same data used to create the contour plane in Figure 4. Iso-surfaces are colored three-dimensional surfaces that are based on the results of contouring. If the data extend to the edges of the space being analyzed the surface will terminate there, if it does not the surface can completely encompass the data. The ranges of values are the same for iso-surfaces with contours and the color spectrum used is the same. Iso-surfaces can be viewed without contours.

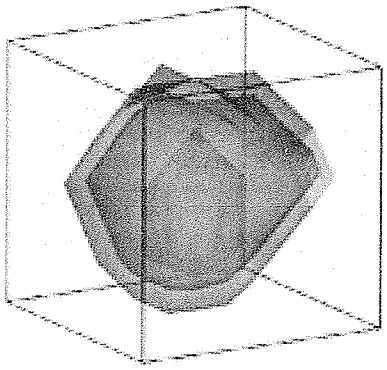

Figure 5: iso-surface

A.5.4. Blanking

A cell is defined as the volume defined by eight neighboring data points. Blanking allows the removal of the graphical representation of cells (Figure 6). For value-blanking conditions can be set to remove cells based on the values held by the data points defining the cell. It is a useful tool when trying to exclude extraneous data during analysis. Other forms of blanking include depth blanking and IJK blanking.

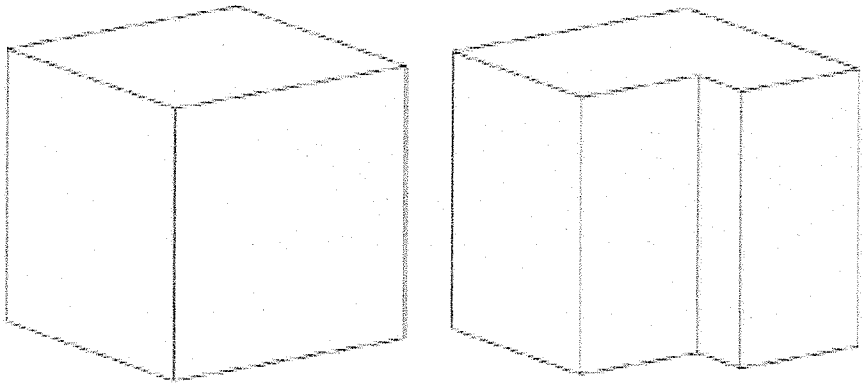

Figure 6: unblanked and blanked volume

A.5.5. Animation

A data file is a collection of zones, each of which describes the atmospheric makeup of the volume for a single time step. Tecplot can take the images produced for each time step and compile them into an animation file. An animation can be viewed to give the

user a sense of time and movement when analysis the data, giving the ability to examine relationships that exist over time more extensively. A succession of contour planes representing the same area over time is depicted in Figure 7.

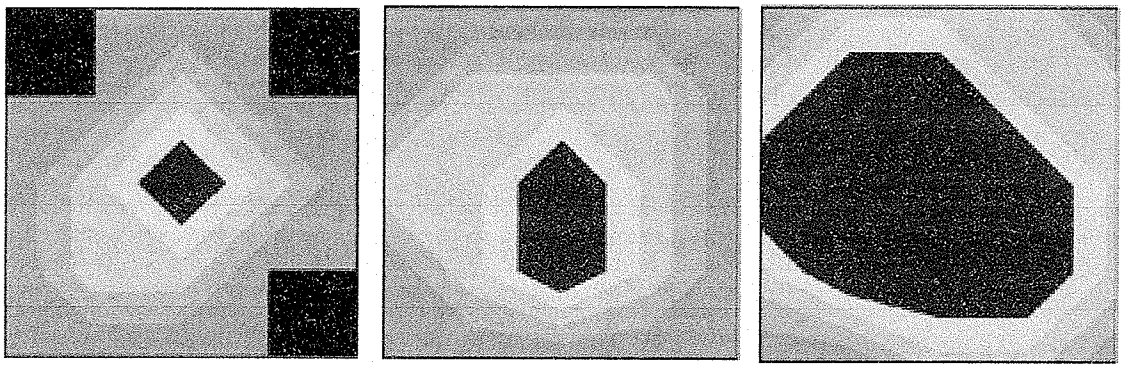

Figure 7: contour planes in a time series

A.6. Developing Graphics and Animation

In an attempt to maximize the effect of using Tecplot to display the results of DDTINDEX a number of steps must be taken. The objective is to arrive at a three-dimensional graphical representation of the DTTINDEX data that is faithful to the GOTHIC model. With the present DDTINDEX output it is not possible. Manipulation of the data file is required, but it is vital that the data not be altered. Considering methods of illustrating the features of the modeled volume, involving its geometry, would add to overall usefulness. Examining the possible visualization methods available to would be valuable in achieving an optimized display.

A.6.1 Expanding data

Concern lies mainly with the results of DDTINDEX. The problem with this data is that it is cell center data, therefore when developing graphics it does not fully represent the volume. By expanding the data a visual model of the subdivide volume can be developed.

To properly represent the entire volume and its cell configuration, the cell center values could be average out to the locations of the vertices. This would be the minimum

requirement to defining all cells for graphic development. While sufficient the issue discovered with this method was that critical values, specifically those at the extremities of the data, could be diffused out during this process. The result would be a loss of valuable information in the analysis of DDT possibility. A solution would be to define these vertices while maintaining the data at the cell center. Under the structure of IJK-ordered data this would not be possible since there would be a loss of consistency over the data structure. Therefore, to maintain an IJK structure the addition of face center, and edge center data would have to be added. Figure 8 illustrates the modification of data from cell center to its expanded state. The result would be the same data structure presented in GOTHIC output, where one cell would be represented by 27 data points.

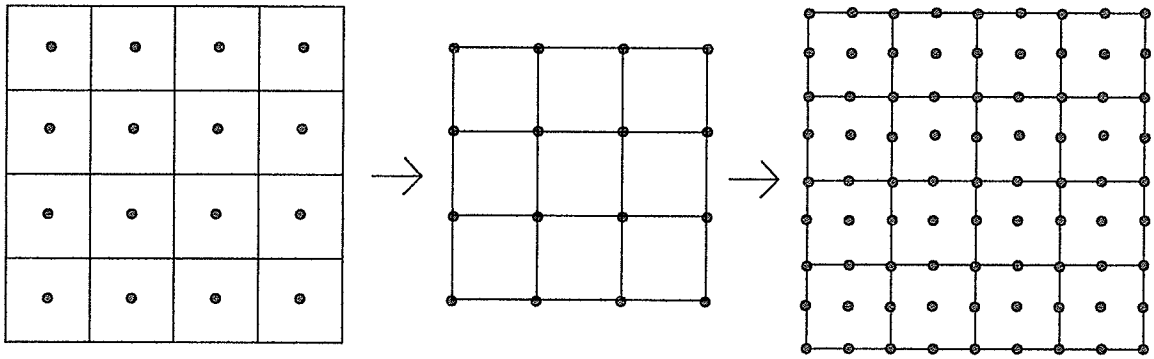

Figure 8: cell center data expansion (two-dimensional)

A number of methods can be incorporated to perform the expansion of data, an inherent issue in all is the addressing of objects. All subdivided volumes are rectangular in nature, however simulated spaces may not allows conform to this convention. As a solution GOTHIC supports the blockage of cells, which prevent the flow of gaseous mixtures. These blockages can be used to simulate interior equipment, walls, or can define the shape of the volume. Within the data file, blocked out cells will be represented by zero or near zero-values throughout the simulation. It is these values that cause difficulty when expanding the data.

As the data are expanded, blockage data will diffuse into nearby data points ultimately affecting the overall results. Therefore, a method must be developed to exclude this data

from the overall expansion. To perform this task it become necessary to map out the geometry of the subdivided volume, by both examining the data graphically and by consulting the model generated in GOTHIC. The results of this mapping can then be used in the expansion process to properly derive results for data points adjacent to blocked out cells.

A.6.2 Three-dimensional Graphing

There is a distinct value for having the ability to plot data in three-dimensions. Spatial relationship can be established. Three-dimensional movements can be recognized. Different techniques can be employed to develop three-dimensional plots for distributions within a volume.

One such technique is through the use of contours. Contours are two-dimensional, but using multiple contour planes in combination can help illustrate the spatial structure of the gas distributions. Examining a series of planes in a single direction can give the viewer a sense of associations across planes (Figure 9a). Combining planes of different orientation can help place emphasis on critical areas, and further enhance the three-dimensional representation of the model (Figure 9b). Employing transparencies and an isometric view can help enhance the impression of volume

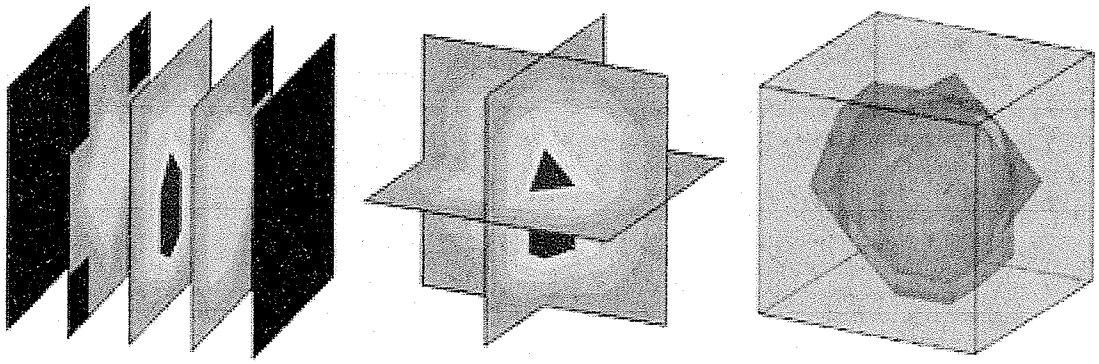

(a) (b) (c)

Figure 9: (a) contour plane series, (b) contour plane combination, and (c) iso-surfaces

Transparencies have become an essential feature when viewing data in three dimensions. In three-dimensional views, transparencies allow users to view multiple layers of data, without removing any information. The recent surge in graphical development has made it easier to produce transparency effects, without substantially increasing the load on processing hardware. Transparencies were added to the latest version of Tecplot.

While the use of contour planes produces an almost psuedo-three-dimensional plot, using iso-surfaces produces a true three-dimensional image of the data (Figure 9c). For data from both DDTINDEX and GOTHIC data, applying iso-surfaces can thoroughly improve the inspection of data. Surrounding regions with a surface can provide clarity when studying the shape and behavior of distributions produced, specifically when trying to distinguish the shape of the clouds of gas. Typically, the cloud makeup is stratified, where the concentrations dissipate from the center or source of the cloud. Applying transparencies to iso-surfaces makes it possible to peer into the interior of a cloud to observe the layering of data.

A.6.3 Using Value-blanking

Blanking is an effective tool for removing graphical data that is unnecessary or may prevent the user from getting a clear view of valuable information. Cells can be blanked by setting conditions based on the values of any property available in the data set. Through value-blanking critical areas in, the data can be highlighted. It was discovered that value blanking could be used to support the volume geometry of the GOTHIC model.

With mapped information of the rectangular gothic volume, a new property could be added to the data file for the purposes of blanking blocked out cells. The nature of the data file required this property exist in all data points and be repeated in each zone. This added property would simply contain one value for data points representing blocked cells and another value for data that existed within the geometry of the model. As demonstrated in Figure 10, the overall effect is the ability to shape the graphical data to best represent the containment structure.

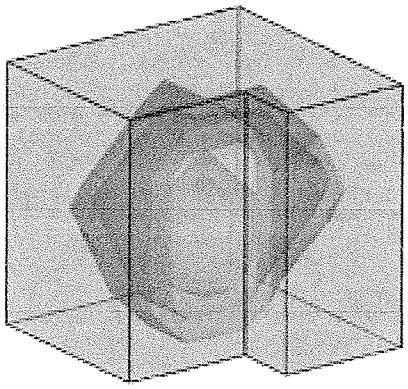

Figure 10: value blanking of data

A.6.4 Adding objects

As zones can be used as a vehicle for the time in the data file, they can also be used to draw lines and shapes to generate interior objects. IJK data are restricted by its ability to represent rectangular data. The finite element format for data is capable of outlining shapes including lines, block and triangles. By applying this to new zones of data replicating the locations stipulated in the IJK data it becomes possible to generate shapes with data points acting as vertices (Figure 11). Using the mesh feature outlines these new zones and using the shade feature generates surfaces produced by these finite element shapes.

Blanking cells is successful at delivering the shape of the model to the viewer, still it can get difficult distinguishing the actual limits of the volume. If the volume maintains the rectangular shape the boundary feature is available, however this method will not work for shapes defined by blanking. Finite element zones can be used to create outlines that emphasizes the boundaries of the model under study. This technique has been employed in Figures 10 and 11.

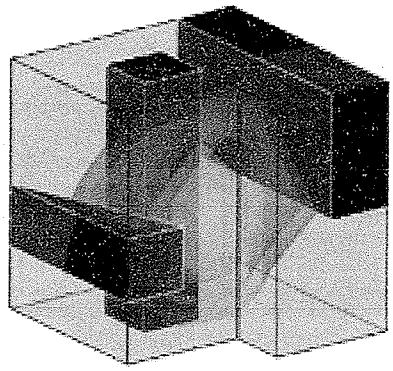

Figure 11: addition of objects

A.6.5 Animating with Macros

Tecplot has a built-in animation generator that can cycle through the existing zones to create an animation over time. This feature can be effective, but once zones are added for outlining and placing shapes this generator becomes insufficient. For further control when generating animations macros can be used. Macros are user built programs that can manage the various features and functions Tecplot offers. This includes the ability to show and hide zones simultaneously. The images produced can be saved as frames of animation and compiled to create an animation file. The end product is an animated presentation that exhibits the geometric features of the model as the data changes frame by frame. Figure 12 is a series of frame from a single animation. The results of this animation were produced by using macros to cycle through the data frames while constantly displaying the borders of the geometry and the objects. Since the time step is user defined the animation file does not co-ordinate with real time. Supported viewing software does allow the viewer to control the animation speed, as well as pausing and stepping through frames.

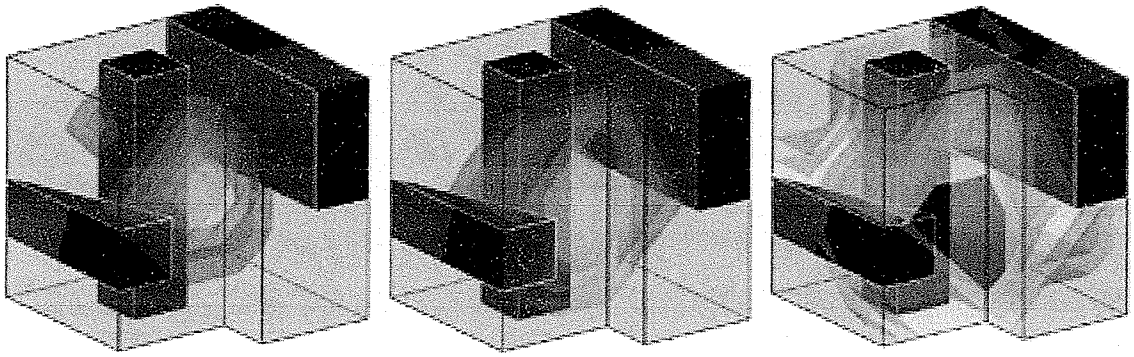

Figure 12: three-dimensional animation with macros

A.7. Effectiveness

There is substantial manual effort necessary to produce these reasonable results. The need to map the volumes and objects, as well as having to develop the graphical features that represent these shapes, can be time-consuming. Mapped results must be applied when expanding the data. Special consideration must be taken at times when interior objects are in contact or in close proximity. Once the zones holding graphical features have been produced, and the expansion method finalized with the mapped information they can be repeatedly used on varying scenarios within the model. If the model is changed or another model is used, it must be remapped.

The combination of plotting data while highlighting geometric features is significant. It not only allows a user to understand the spatial relationships within the gas flow, but tie in these patterns with the characteristic of its physical containment. Because the geometry is actually of the model generated in GOTHIC, it is restricted to the cell structure of the data. Though, considered misleading, it would be possible to add models of more detailed objects and volumes.

Overall, the method of using the combination of iso-surfaces and transparencies gives the best sense of space, since it produces three-dimensional products that can easily be associated with gas clouds. In animation files it also gives the clearest graphical representation of movement and scale. The largest issue with this display technique is the

limitations of transparencies. With multiple surfaces in layers what is transparent will eventually become opaque, making it difficult or impossible to observe critical areas within the data. It is possible to increase the level of transparency, but increasing this too much will leave outside data in distinguishable. Intuitively, viewers assume there to be a stratum of data, with an outward diffusion of gas concentration. Therefore, with a generalization of a cloud, by instinct it is understood that data becomes closer to critical or more critical with proximity to its heart. Intuition, however is vague.

Generalizations made with and iso-surface based animation can be used for more in-depth analysis. By pinpointing possible critical areas, a user can focus the graphical study to these areas. Reducing the number of iso-surfaces can help making key attributes more visible. Applying contour planes that intersect critical areas is also effective at highlighting important data.

A number of different methods is available to graphically represent both GOTHIC and DDTINDEX. What is considered most effective is dependent on the situations the simulations produce and the intended use of these graphics.

Appendix B:

VRML Combustion Simulation

Introduction

Virtual Reality Modeling Language (VRML) is the main tool used for this research and combustion analysis.

Combustion

Combustion analysis is a vital component in research and design. Analysis tools have been designed to help simulate combustion behavior and add clarity to varying situations. Extensive examination can be conducted with CFD or similar codes, and visualization packages can be used to conduct scientific inquiry. Codes such as FLUENT® and graphic software like TECPLOT® are readily available for this form of analysis. While examinations such as this can be very thorough, they can also be expensive and time consuming. This expenditure often cannot be justified.

In many cases extensive studies of combustion system behavior is not as vital as the development of a general understanding of the patterns formed. By generalizing relationships it is possible to construct a simplified model of a system that provides the user with the necessary information quickly and efficiently. Observing flame propagation during a combustion simulation can provide an overview of the overall behavior of the system.

VRML

VRML is a scripting language specifically designed for developing web-based VR environments and applications. The language is able to construct three-dimensional geometry, transformations and interactivity.

As with all scripting languages, a viewer is necessary for using VRML. The selected viewer is Cosmo Player 2.1, from Cosmo Software (Figure 1). Supported is VRML 2.0.

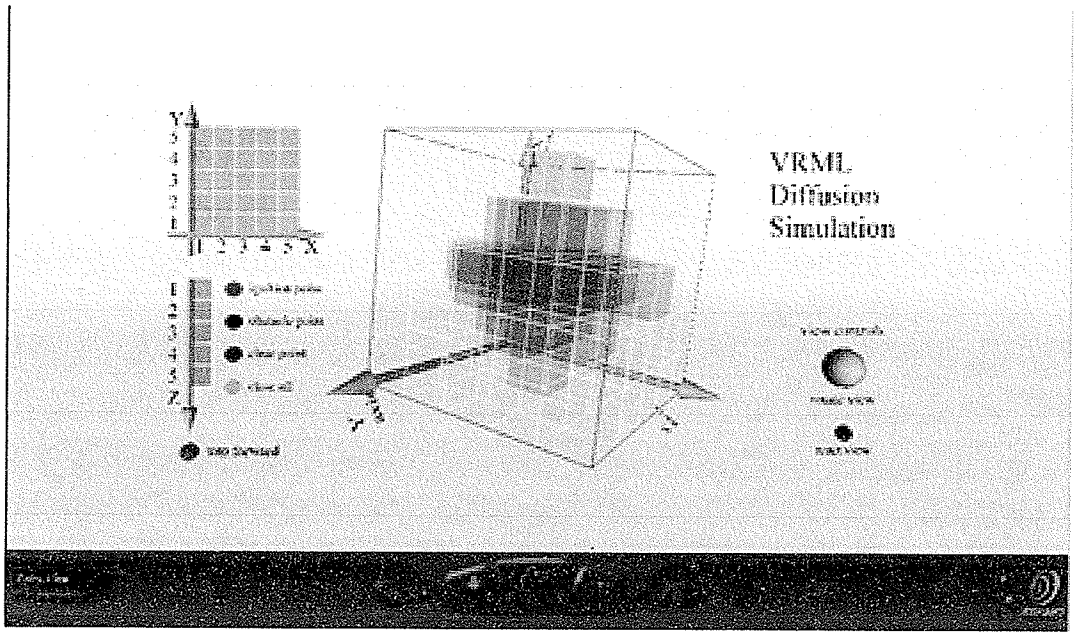

Figure 1: Cosmo Player plug-in

Combustion analysis results have been visualized with VRML because of the freedom the scripting language gives for both viewing and distribution. It has demonstrated it is capable of recreating environments and physical relationships. Using VRML may be an effective tool for generating a flame propagation simulation in a three-dimensional environment.

JavaScript

By pairing VRML with JavaScript, further functionality can be added to the generated environments. JavaScript is a scripting language commonly used with other web tools to

add interactivity and other functions to websites. While JavaScript is not as powerful as Java, it is still very capable and widely accepted.

Implementation

Only the flame propagation of a combustion system will be considered, but even this is a complex field of study. Thus, to first investigate the possible methods for implementing this form of simulation into a VRML environment, a simplified model of flame propagation must be considered.

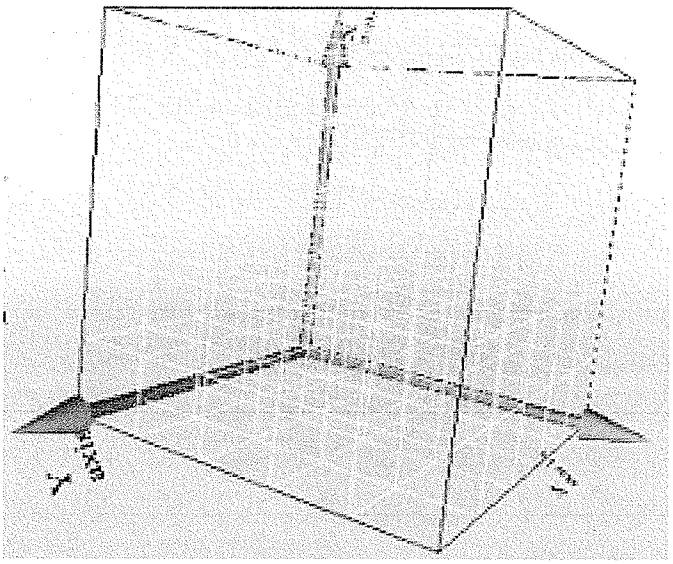

Figure 2: three-dimensional grid (5 x 5 x 5)

The method considered is a cellular approach with the environment being a three-dimensional grid (Figure 2). Each cell will be a cube. The size of the grid selected for this example is five by five by five, therefore composed of 125 cells. One cell is selected as an ignition point and from there the flame will propagate. As the flame propagates the cells become activated to signify its growth. A color change in the cell is used to signal that it has become active.

The simplified model for flame propagation is achieved by first considering the ignition cell and by activating the cells next to itself in the six normal directions. These recently

activated cells are now considered. If any of the six face-adjacent cells to these are not already part of the flame, they are activated (Figure 3). This happens at each step of the simulation. Users are given control as to when the simulation moves forward (ie. step by step). This process produces a general impression of flame growth.

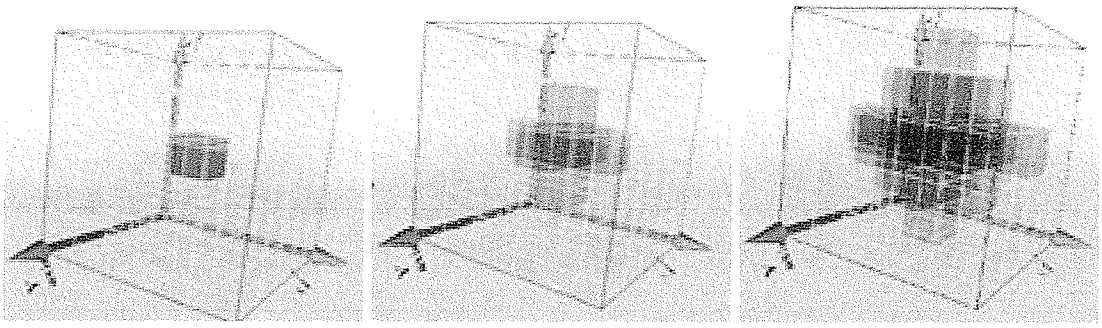

Figure 3: cellular flame growth

Another condition to the propagation is the presence of obstacles. How a flame behaves in the presence of obstructions is crucial to its overall behavior. Propagation complexity increases in these situations. For the purpose of this application the flame growth merely navigates around obstacles. Obstructions are defined as cells within the grid.

Features

There are two versions of the program. Common to both versions is the ability to place ignition points at any location within the grid. This is conducted through an interface that allows the user to select an x and y locations, followed by a z co-ordindate, all of which correspond to cell locations within the simulation grid (Figure 4). From the ignition point a touch sensor is used to step through the simulation in stages as it is pressed. Also, common to both are controls can manipulate the orientation of the three-dimensional grid, to improve observability (Figure 5).

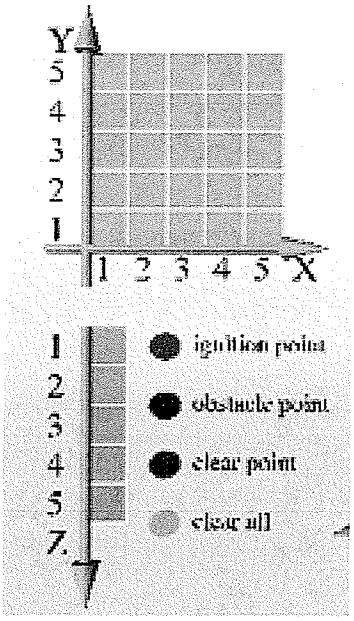

Figure 4: Location selector

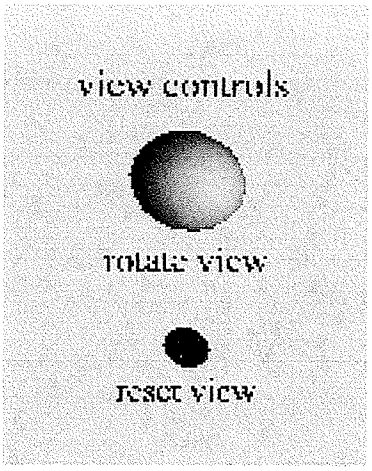

Figure 5: View controls

The first version of the simulation allows the user to place obstacles within the grid by selecting cells and establishing them as barriers. This process uses the same interface as the ignition selection. In this version the ability to clear cells in the same manner has also been added.

The second version presents the grid with established obstacles. Three situations are given, a menu is provided to select between the three. While, the user can still select ignition locations the ability to add obstructions has been removed.

Conclusion and Further work

A general understanding can be derived from this representation of flame propagation, but it is oversimplified. A true sense of flame mechanics cannot be found in this model. The result is closer to a straightforward diffusion model than that of a flame. What this simulation does provide is the development of a visual technique and an interface that can be adapted to more complex applications. The complex physical relations must be further

deconstructed into a form that is useable by these tools. The hope is that the overall result is a functional simulation that can be used in design and analysis.

The development of this simulation has proven a valuable experience, especially because of the practical exposure to VR concepts and the ability to apply them to our field of study. Based on this project, and others, it becomes easy to see the wide variety of applications that VR can be applied towards. The nature of this simulation prevents the use of other tools, including VR specific applications, and CAD programs that can construct VRML code. It is my hope that future work with combustion analysis will involve these applications. Still, working closely with VRML and JavaScript has provided an appreciation for the capabilities presented by these scripts. As a practice in the use of VRML, and development a VR application, this research has performed its task.